

High-speed imaging of glutamate release with genetically encoded sensors

Céline D. Dürst¹, J. Simon Wiegert^{1,4}, Nordine Helassa^{2,5}, Silke Kerruth^{2,6}, Catherine Coates², Christian Schulze¹, Michael A. Geeves³, Katalin Török² and Thomas G. Oertner^{1*}

The strength of an excitatory synapse depends on its ability to release glutamate and on the density of postsynaptic receptors. Genetically encoded glutamate indicators (GEGIs) allow eavesdropping on synaptic transmission at the level of cleft glutamate to investigate properties of the release machinery in detail. Based on the sensor iGluSnFR, we recently developed accelerated versions of GEGIs that allow investigation of synaptic release during 100-Hz trains. Here, we describe the detailed procedures for design and characterization of fast iGluSnFR variants *in vitro*, transfection of pyramidal cells in organotypic hippocampal cultures, and imaging of evoked glutamate transients with two-photon laser-scanning microscopy. As the released glutamate spreads from a point source—the fusing vesicle—it is possible to localize the vesicle fusion site with a precision exceeding the optical resolution of the microscope. By using a spiral scan path, the temporal resolution can be increased to 1 kHz to capture the peak amplitude of fast iGluSnFR transients. The typical time frame for these experiments is 30 min per synapse.

Introduction

One of the fundamental parameters determining synaptic strength is the release probability of the presynaptic bouton. Release probability is classically assessed in electrophysiological recordings from the postsynaptic neuron. In the neocortex and hippocampus, however, two neurons are frequently connected by more than one synapse, which makes it very difficult to achieve a situation in which responses from a single synapse can be electrophysiologically isolated. Furthermore, both presynaptic changes (vesicle depletion and changes in release probability) and changes on the level of postsynaptic receptors (e.g., phosphorylation, desensitization, saturation, lateral diffusion, and internalization) contribute to the variability of postsynaptic responses^{1,2}. These effects become even more difficult to disentangle during high-frequency stimulation, when all physiological parameters change simultaneously as the synapse struggles to maintain transmission. Owing to these complications, it is an attractive proposition to assess synaptic physiology with functional imaging methods, as they convincingly isolate responses from a single synapse even if other synapses on the same neuron are active at the same time. Whereas a large number of imaging studies used postsynaptic Ca^{2+} transients as a readout of synaptic efficacy, it is now possible to intercept synaptic transmission at the level of cleft glutamate, effectively isolating presynaptic dynamics from postsynaptic changes.

Overview of optical glutamate sensors

In the past decade, two types of optical glutamate sensors have been developed: chemically labeled sensors and GEGIs. Both types of sensors utilize a glutamate-binding protein that is either labeled with a synthetic fluorophore or fused to a fluorescent protein. Sensors based on the ligand-binding domain of an AMPA receptor (AMPA) subunit conjugated with a small fluorescent dye molecule near the glutamate-binding pocket have been used to image bulk extrasynaptic glutamate dynamics in the brain^{3,4}. A chemical Förster resonance energy transfer (FRET)-based approach, combining a donor and acceptor fluorophore with the glutamate-binding protein iGluR5-S1S2 (Snifit-iGluR5)⁵ showed an improved fluorescence change in cultured cells but has not yet been applied to brain tissue.

¹Institute for Synaptic Physiology, Center for Molecular Neurobiology Hamburg, Hamburg, Germany. ²Molecular and Clinical Sciences Research Institute, St George's, University of London, London, UK. ³School of Biosciences, University of Kent, Canterbury, UK. ⁴Present address: Research Group Synaptic Wiring and Information Processing, Center for Molecular Neurobiology Hamburg, Hamburg, Germany. ⁵Present address: Department of Cellular and Molecular Physiology, Institute of Translational Medicine, University of Liverpool, Liverpool, UK. ⁶Present address: Department of Biophysical Chemistry, J. Heyrovský Institute of Physical Chemistry, Prague, Czech Republic. *e-mail: thomas.oertner@zmnh.uni-hamburg.de

Sparse and cell-specific labeling without background fluorescence, a precondition for single-synapse studies, seems to be difficult to achieve with chemically labeled sensors.

The first fully GEGI, called FLIPE⁶, was FRET-based and contained a glutamate-binding protein (GltI from *Escherichia coli*)^{located} between an N-terminal enhanced CFP (ECFP) and a C-terminal YFP called Venus. Later improved to reach a maximum CFP/YFP ratio change of 44% and a dissociation constant (K_d) of 2.5 μM ^{7,8}, the sensor SuperGluSnFR allowed measurements of the time course of synaptic glutamate release and spillover in hippocampal cultures. However, the signal-to-noise ratio (SNR) of SuperGluSnFR was still low, and ~30 traces had to be averaged to measure glutamate release in response to single action potentials (APs). A substantial improvement was the development of iGluSnFR⁹. iGluSnFR is an intensity-based glutamate sensor constructed from *E. coli* GltI and circularly permuted enhanced GFP. Its high fluorescence dynamic range ($\Delta F/F_{\text{max}}$ of 4.5) and K_d of ~4 μM make it a very suitable tool for investigating cleft glutamate dynamics. iGluSnFR has been used to measure glutamate in a variety of tissues, such as the retina¹⁰, visual cortex¹¹, and olfactory bulb¹². We and others developed variants displaying different kinetics, affinities, and emission profiles^{13–15}. Those new GEGIs with varied biophysical properties enable researchers to select the most appropriate sensor depending on the biological question (bulk tissue versus single synapse) and imaging system (camera, galvanometric laser scanner, or resonant scanner).

Comparison with other methods to image presynaptic function

To image presynaptic function, fluorescent glutamate sensors are not the only possibility. The change in vesicular pH during vesicle exocytosis and recycling/reacidification has been successfully exploited to measure the activity of individual presynaptic terminals. SynaptopHluorin, the first genetically encoded pH indicator, was based on a pH-sensitive GFP variant fused to the C terminus of synaptobrevin/VAMP2 to target the sensor to the inner surface of synaptic vesicles¹⁶. Other vesicular-targeting strategies used fusion to synaptophysin¹⁷, synaptotagmin¹⁸, and the vesicular glutamate transporter VGLUT¹⁹. Spectrally red-shifted sensors with a red fluorescent pH-sensitive protein such as VGLUT-mOrange2 (ref. ²⁰) and sypHTomato²¹ were developed, and the ratiometric sensor Ratio-sypHy²² was instrumental in showing the arrested development of synapses in dissociated neuronal culture. In addition, in primary cultures, pHluorins are sufficiently sensitive to detect single-vesicle release events^{23–25}. It is even possible to localize individual fusion events with a precision exceeding the resolution limit of the microscope²⁶. Analysis of release during high-frequency activity, however, is difficult with pH-based methods: reuptake and reacidification are slow processes, leading to rapid accumulation of green fluorescence inside active synaptic terminals. Furthermore, pH-based indicators provide no information about the glutamate content (filling state) of individual vesicles. Another technique for studying presynaptic function is to image the loading and unloading of amphiphilic styryl dyes (FM dyes), initially developed to study vesicle recycling at the neuromuscular junction²⁷. The lack of cellular selectivity prevents the use of FM dyes at individual synapses in the densely packed neuropil. In addition, the relatively long partitioning time of FM dyes in and out of the membrane (seconds) renders the relation between staining/destaining events and sub-millisecond glutamate release rather obscure.

Overview of the procedure

The Procedure can be divided into two sections (Fig. 1); sensor development (Steps 1–44) and functional imaging of synaptic activity in hippocampal slice cultures (Steps 45–62).

Sensor development (Steps 1–44)

Although iGluSnFR is an excellent general-purpose GEGI, it may be necessary to further optimize specific properties, such as affinity for glutamate (K_d), brightness, or kinetics, for specific experiments. Optimization starts with structure-guided mutations of residues close to the glutamate-binding pocket (Fig. 1a) (Step 1). Newly generated variants are expressed in *E. coli*, purified, and tested in vitro for glutamate-induced changes in fluorescence (Steps 2–20). If the dynamic range is deemed sufficient, affinity and kinetics are determined by stopped-flow fluorimetry (Steps 21–37). The most promising candidates are expressed and characterized in HEK cells (Steps 38–42) and, finally, in neurons (Steps 43–62). We found considerable differences in the absolute affinity and kinetics of sensor molecules in solution, as compared to those of the same molecules tethered to the plasma membrane of cells¹³. Relative differences between GEGIs, however, were conserved, validating the use of in vitro calibrations for sensor optimization.

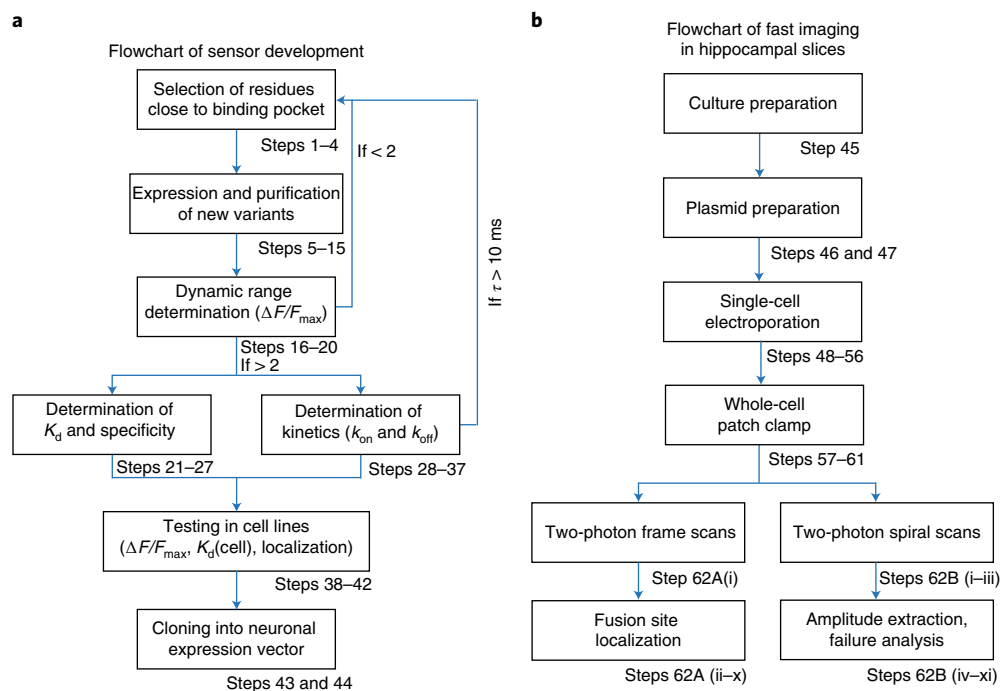


Fig. 1 | Overview of the protocol workflow for the development of glutamate sensors and two-photon imaging of glutamate transients in individual synapses. a, Flowchart of sensor development. **b**, Flowchart of fast imaging in hippocampal slices.

Imaging synaptic function (Steps 43–62)

Single-cell electroporation is the method of choice to achieve very sparse expression of glutamate sensors in organotypic culture of brain tissue (Fig. 1b) (Steps 46–56). The sparse expression makes it easy to follow the axon of a patch-clamped sensor-expressing neuron to a distal projection area, e.g., cornu ammonis 1 (CA1). Although camera-based systems are ideal for functional imaging in dissociated neuronal culture, two-photon microscopy is typically used to detect weak functional signals deep in scattering tissue (Steps 57–62). The optimal strategy for functional imaging depends on the goal of the experiment: to obtain spatial information about the fusion sites of vesicles on individual presynaptic boutons, we use fast frame scans and slower GEGIs (iGluSnFR) (Step 62A). To accurately determine the amplitude of individual glutamate transients, a prerequisite for optical quantal analysis, spiral scans on individual boutons provide increased temporal resolution and better SNR (Step 62B). Although 500 Hz provides sufficient temporal resolution for iGluSnFR imaging, we increase the spiral scan frequency to 1 kHz for ultrafast GEGIs.

Limitations of the method

Glutamate diffuses out of the synaptic cleft in <1 ms. Even the fastest GEGIs cannot monitor the true kinetics of free glutamate diffusion because the sensor needs time to rearrange its conformation to become fluorescent. In addition, scanning microscopy has limited temporal resolution. For capturing sub-millisecond fluorescence changes, it would be necessary to park the excitation beam on the synaptic cleft. This is not a technical problem, but in practice, point-scan experiments are extremely sensitive to small lateral movements of the active bouton in the tissue. At the moment, galvanometric scanning can still adequately sample the fastest GEGIs.

The number of trials that can be obtained from a single bouton is limited by the unavoidable bleaching of the indicator molecules and eventual destruction of the release machinery by toxic photoproducts (e.g., oxygen radicals). Therefore, the laser exposition per single AP should be reduced to a minimum. To measure GEGI transients in response to individual APs, we image in spiral mode for ~80 ms. We routinely acquire ~100 trials from single boutons without any decay in amplitude or release probability (see the ‘Experimental design’ section and Supplementary Fig. 1c). By using lower laser power, this number can be extended to 200 trials at the cost of a slightly lower SNR. Longer intervals between trials allow replenishing indicator molecules by lateral diffusion,

but this strategy is limited by the need for stable whole-cell access during the entire experiment for reliable AP generation.

Experimental design

Development and characterization of fast glutamate probes

Site-directed mutagenesis and protein expression/purification are done by following standard procedures and should lead to high yields of the GEGIs, with a purity >90% in a single-step purification process (determined by SDS-PAGE). One of the most important parameters is the fluorescence dynamic range $((F_{+glu} - F_{-glu})/F_{-glu})$, which is a measure of the fluorescence change upon glutamate binding. If the dynamic range of the new GEGI variant is <2, the probe's response to glutamate is not high enough to be suitable for cellular experiments.

The affinity of the GEGI, expressed as K_d , must be appropriate for the expected glutamate concentration in the cellular or tissue environment. If the goal of the experiment is to distinguish synaptic failures (no glutamate release and no GEGI signal) from successes (stimulation-induced glutamate release), a very high affinity is desirable. If a linear response is important, e.g., to estimate the number of vesicles released simultaneously, a slightly lower affinity might be advantageous. For a GEGI to be a useful probe for *in vivo* imaging, it also needs to be specific for glutamate. Therefore, binding to other ligands must be assessed (Fig. 2a). As iGluSnFR is based on the glutamate/aspartate ABC transporter protein (GltI), it is expected that the sensor will retain a substantial affinity for aspartate. However, it should be unresponsive to serine or glutamine. Most of the GEGIs indeed show a fluorescence response to aspartate binding, sometimes even with a higher fluorescence dynamic range than that for glutamate. However, the affinity is often lower, and, fortunately, aspartate does not act as a neurotransmitter. Nevertheless, aspartate sensitivity must be considered when monitoring glutamate in non-neuronal tissues or cellular compartments.

To observe fast events, such as neurotransmission in synapses, the kinetics of the formation and decay of the fluorescence state are critical. Thus, the association and dissociation of the purified GEGIs are determined *in vitro* by stopped-flow fluorimetry (Fig. 2b). While performing association measurements, it is essential to record baselines for the buffer to obtain the zero level of the photomultiplier tube (PMT) and for obtaining the starting point of the fluorescence increase of the glutamate-free GEGI. This recording is essential to detecting rapid phases (>1,000/s) that are faster than the resolution of the stopped-flow device (~1-ms mixing time) and thus appear as jumps. Recording the dissociation of glutamate from the GEGIs is especially challenging, as the glutamate must be removed from the sensor, which is difficult due to lack of chemical traps. We circumvent this obstacle by mixing the glutamate-bound GEGI with the high-affinity GluBP 600n ($K_d \sim 600$ nM)⁶. However, for low-affinity variants, these measurements are limited by the concentration of GluBP 600n available and by the very small decrease in fluorescence amplitude. Low-affinity GEGIs ($K_d > 1$ mM) must be saturated with glutamate concentrations in the millimolar range; however, GluBP 600n is at best concentrated to be ~1 mM in the optical cell. As only a small fraction of the GEGI is dispossessed of its glutamate, only a very small decrease in fluorescence occurs and, thus a small signal is observed.

For *in vivo* use of the GEGIs, the sensors must be attached to the outer membrane of a cell. Thus, the sensors are cloned in mammalian expression vectors, which add a mouse Ig κ -chain for secretion and a platelet-derived growth factor receptor (PDGFR) transmembrane helix for membrane attachment. To confirm correct localization, the sensor is expressed in cell lines (HEK293T cells) and titrated with glutamate to determine the cellular K_d . We found that the attachment to the outer membrane of the cell increases the variants' affinity for glutamate by a factor of up to 20-fold. Relative differences between the variants, however, are conserved¹³. This affinity increase must be considered when choosing a suitable sensor for *in vivo* applications.

Imaging synaptic glutamate release with two-photon microscopy

For expression in neurons, we clone the GEGIs behind the human synapsin 1 promoter and electroporate single neurons in organotypic slice cultures of rat hippocampus. GEGIs are relatively dim in the absence of glutamate, making it difficult to focus on small structures such as axonal boutons. We routinely use co-expression of a bright RFP (tdimer2 or tdTomato) to label the cytoplasm and follow the axon through the tissue; the newly developed CyRFP1 (ref. 28) is also an excellent choice for this purpose. The red fluorescence also provides additional information about the volume of individual boutons. Electroporated CA3 neurons are clearly visible under a stereomicroscope (5× objective,

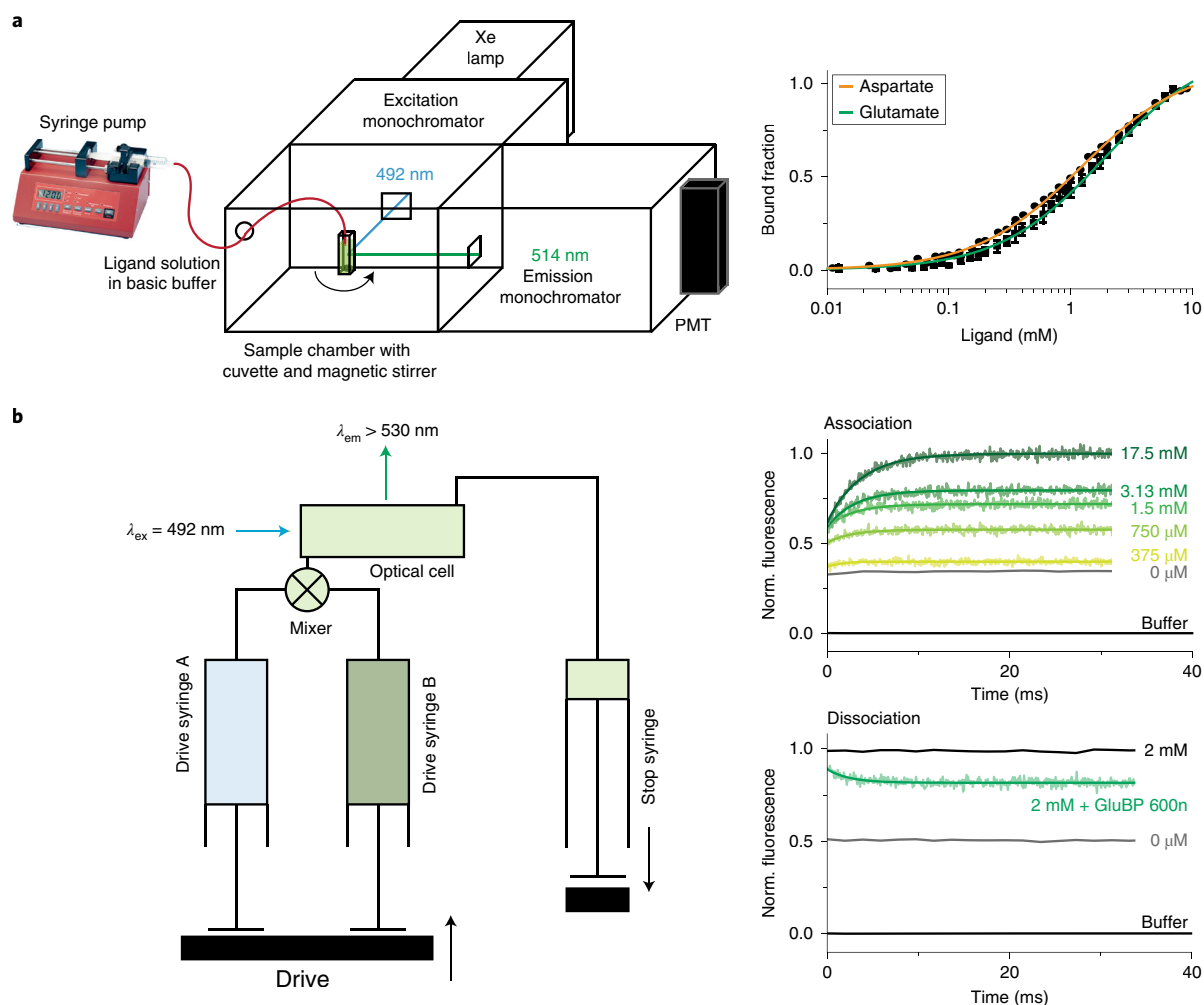


Fig. 2 | Characterization of GEGIs. **a**, (Left) Setup for affinity and selectivity determination. GEGI in assay buffer is placed into a fluorescence cuvette with a magnetic stirrer and placed inside the sample chamber of the fluorescence spectrometer. With an Aladdin pump, the ligand (Glu, Asp, and Ser) is continuously added to the cuvette while the fluorescence is recorded ($\lambda_{\text{ex}} = 492 \text{ nm}$, $\lambda_{\text{em}} = 514 \text{ nm}$). (Right) Examples of affinity curves of a GEGI for glutamate (black squares) and aspartate (black circles). The fluorescence emission is corrected for dilution and bleaching and plotted against the glutamate concentration in the chamber. The data are then fitted with a Hill equation (green and orange traces for glutamate and aspartate, respectively). **b**, (Left) Setup for stopped-flow kinetic measurement. The solutions are rapidly mixed in the mixing chamber and then pushed into the optical cell, where the fluorescence is excited at 492 nm and emission is detected by a photomultiplier tube with a cutoff filter ($>530 \text{ nm}$). For association, the GEGI in assay buffer without glutamate is loaded into drive syringe B and mixed with assay buffer containing increasing concentrations of glutamate loaded into drive syringe A. For dissociation, the GEGI in assay buffer with saturating glutamate concentration is loaded into drive syringe B and mixed with GluBP 600n in assay buffer loaded into drive syringe A. For both measurements, the PMT zero level is determined by mixing identical solutions (assay buffer with assay buffer), and the intrinsic fluorescence of the GEGI is recorded by mixing the GEGI in assay buffer with assay buffer (both without Glu). (Right) Examples of recorded time traces. (Top) Fluorescence increase observed when GEGIs are mixed with increasing glutamate concentrations. (Bottom) Decrease in fluorescence when glutamate is retained from GEGI by GluBP 600n. The raw data are fitted with mono-exponential decays (dark-green line).

DsRed filter set) 2–4 d after electroporation (Fig. 3a,b). Two-photon excitation at 980 nm reveals membrane localization of the GEGI (Fig. 3d) as well as axons and boutons of the expressing neurons in CA1 stratum radiatum, far away from the somata in CA3 (Fig. 3c). Targeted patch-clamp recording from a transfected neuron allows triggering of single APs by brief depolarizing current injections (Fig. 3e). Simultaneous imaging of a single bouton (spiral scan path at high zoom reveals green fluorescence transients time-locked to the APs, indicating glutamate release from the stimulated bouton. In spite of reliable AP generation, synapses frequently failed to release glutamate (Fig. 3e, gray traces), indicating a stochastic vesicle fusion process.

Fusion site localization

Although spiral scans are optimal for determining the peak amplitude of the glutamate signal, we use fast frame scans (16×16 pixels, frame rate = 62.5 Hz) to localize the probable location of the fusing

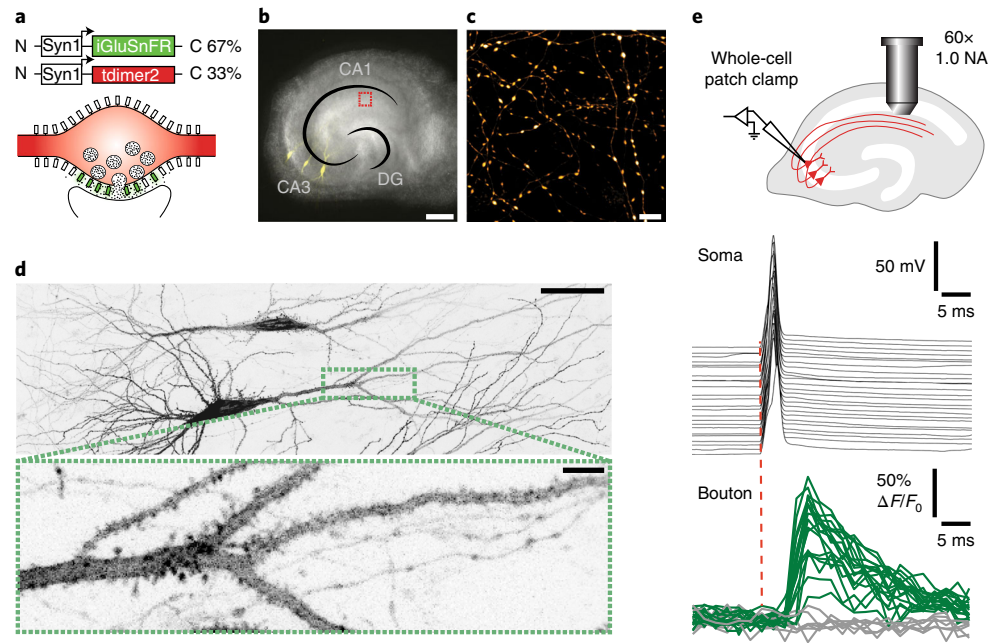


Fig. 3 | iGluSnFR expression in CA3 pyramidal cells in an organotypic slice culture of rat hippocampus. **a**, Co-expression of two plasmids in individual CA3 pyramidal cells in an organotypic slice culture. The RFP tdimer2 labels the axoplasm, and the membrane-anchored iGluSnFR is exposed to the extracellular space. **b**, Transmitted light image (dark field) of a transfected organotypic culture merged with a wide-field fluorescence image showing three transfected CA3 neurons (yellow). The area for synaptic imaging is indicated (red dashed box). Scale bar, 500 μm . **c**, Two-photon image stack (maximum-intensity projection) of CA3 axons in CA1 stratum radiatum (cells not identical to **b**). Scale bar, 10 μm . **d**, Maximum-intensity projection of two-photon images of a CA3 pyramidal neuron expressing iGlu_u 4 d after electroporation (fluorescence intensity is shown as inverted gray values). iGlu_u shown here and other GEGIs had their fluorescence mainly localized to the plasma membrane over the entire cell. Scale bar, 50 μm (top image) and 5 μm (bottom image). **e**, APs are elicited in a transfected neuron by somatic current injections, and glutamate release is simultaneously optically recorded (GEGI fluorescence) from a single Schaffer collateral bouton in CA1, showing a broad distribution of amplitudes and occasional failures. Images were acquired at 500 Hz at 34 °C. Individual trials are classified as successes if the peak amplitude of the GEGI transient is $>2\sigma$ (green traces) and as failures when the peak amplitude is $<2\sigma$ (gray traces). Note the propagation delay between presynaptic APs and glutamate release events at the distal bouton. DG, dentate gyrus; NA, numerical aperture; Syn1, synapsin 1.terminal. **c,e** reproduced with permission from Helassa et al.¹³, National Academy of Sciences.

vesicle in individual trials. The spatial peak of the averaged signal does not necessarily occur in the center of the bouton (Fig. 4a), but is often close to the edge (Fig. 4b), reflecting the random orientation of the synaptic cleft on the surface of the bouton. To localize individual fusion events in noisy images, we fit a 2D Gaussian kernel (Fig. 4c) to the first frame after stimulation. Plotting the center positions of Gaussian fits (Fig. 4c) relative to the morphological outline of the bouton (red channel) showed a small region of release, the active zone (Fig. 4d). Increasing the extracellular Ca^{2+} concentration from 1 to 4 mM did increase the amplitude of single-trial responses, but not the size of the apparent active zone (Fig. 4e). The higher cleft glutamate concentrations caused by single APs in 4 mM Ca^{2+} suggest the simultaneous release of multiple vesicles or a switch from partial to full release. No clustering was found when we fitted green fluorescence before stimulation or in trials classified as failures (Fig. 4f,g).

Spiral scans and amplitude extraction

As we do not know a priori where on the bouton the highly localized and short-lived GEGI signals will appear (Fig. 5a), we must sample the entire surface of the bouton as quickly as possible. Traditional raster scanning (Fig. 5b) requires extreme acceleration of the scanning mirror at the end of each scan line, limiting the maximum frame rate to ~ 120 Hz. By scanning in a spiral pattern, we are able to sample the same area at frequencies of up to 1 kHz. The point-spread function (PSF) of our two-photon microscope is 0.5 μm in the imaging plane and 1.7 μm along the optical axis (full width at half maximum (FWHM), measured with 170-nm fluorescent beads). As the PSF elongates in the axial direction, we sample the upper and lower surface of the bouton simultaneously. Our goal is to extract the amplitude of fluorescent transients from spiral scans independent of the exact position

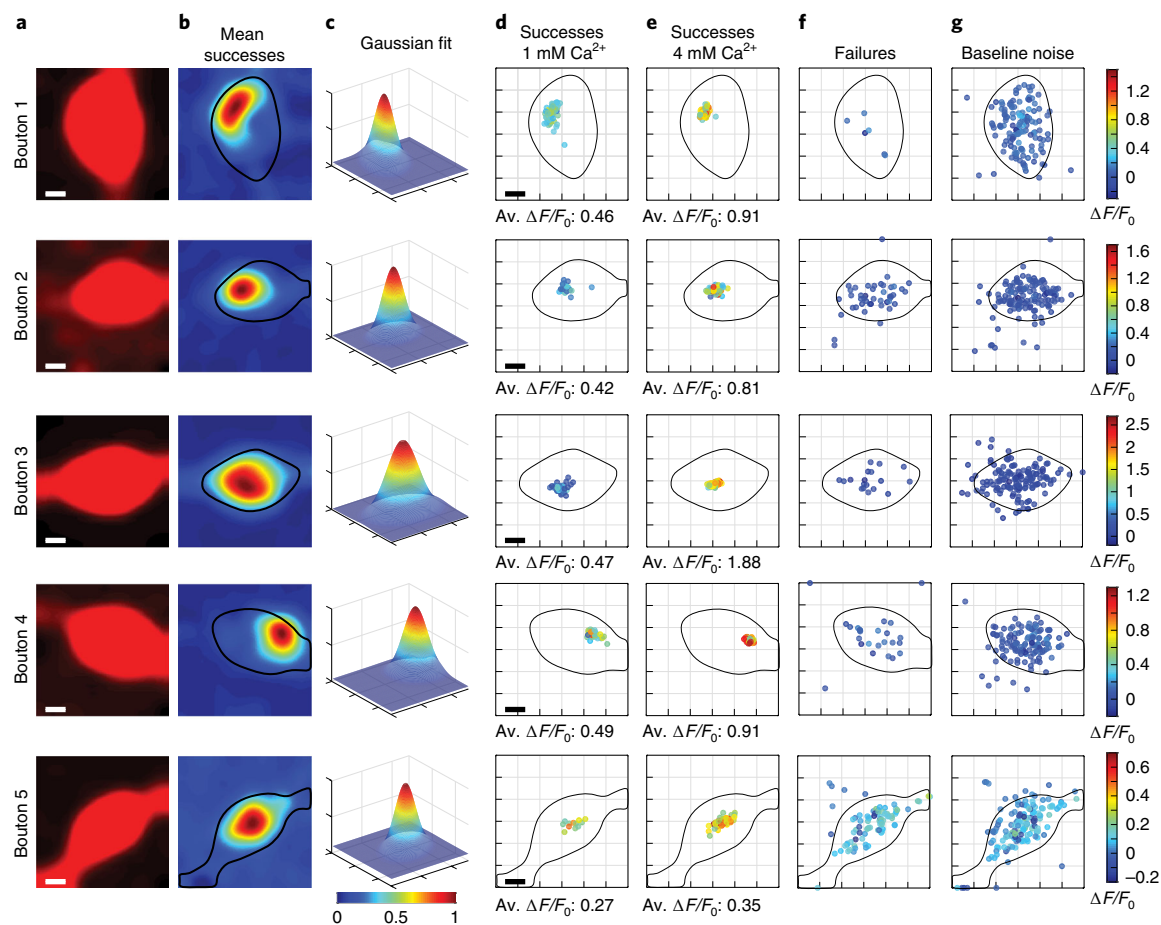


Fig. 4 | Localization of fluorescence transients in low and high $[Ca^{2+}]_0$. **a**, Morphology of individual boutons. Red fluorescence was upsampled (16×16 pixels to 128×128 pixels), aligned, and averaged over all trials. **b**, Average response of iGluSnFR superimposed with bouton outline (black line) from the red channel (morphology). The bouton outline was generated by thresholding the red channel, followed by smoothing. **c**, 2D Gaussian fit to average response. On average, the full width at half maximum (FWHM) was 763 ± 29 nm ($n = 12$; five boutons shown here). **d**, Plotting the center position of 2D Gaussian fits to individual trials. Fusion appears to be localized to a small region on the bouton (active zone). Amplitude ($\Delta F/F_0$) of individual trials is color-coded. **e**, Increasing the extracellular Ca^{2+} concentration increased the amplitude of individual responses, but did not lead to release events outside the active zone. **f**, Fitting responses classified as failures ($<2\sigma$ of baseline noise) did not reveal any clustering, indicating that there was indeed no localized signal in these trials (true negatives). **g**, Fitting frames before stimulation (green baseline fluorescence) also did not result in clustering. Scale bars, $0.5 \mu\text{m}$. Av., average.

of the fusion site on the bouton. To do so, the unfolded spiral scans are plotted as straight lines underneath each other, resulting in a space–time plot (Fig. 5c). Typically, the spiral scan intersects the diffusing cloud of glutamate two or three times per scan, resulting in multiple ‘hot spots’ that all contain information about the same release event. To extract amplitude information, columns (corresponding to positions on the bouton) are sorted according to the change in fluorescence (Fig. 5d). The columns with the largest signal ($\Delta F > \Delta F_{\text{max}}/2$) are averaged (ROI). In trials in which no fluorescence change is detected (failures), the same columns as in the last ‘success’ trial are analyzed. As opposed to a static ROI, this analysis procedure is robust against minute drift of the tissue between trials and does not require a priori knowledge of the fusion location. We extract the amplitude from the resulting fluorescence trace by fitting a single exponential function to the decay of the fluorescence transient. To estimate the noise level (photon shot noise) in each experiment, we perform the same fitting procedure to a section of the baseline (before stimulation). As expected, the baseline amplitudes are close to zero (Fig. 5f, gray dots and columns). Typically, the histogram of all responses (green) also shows one cluster around zero (failures of release); the remaining responses (successes) form an asymmetric, broad peak between 40 and 160% $\Delta F/F_0$. A close inspection of the spatial distribution of the signal (Fig. 5e, average of ten successes) shows a rapid decay of the peak, but no lateral spread, as might be expected from a diffusion process. It is important to note that the

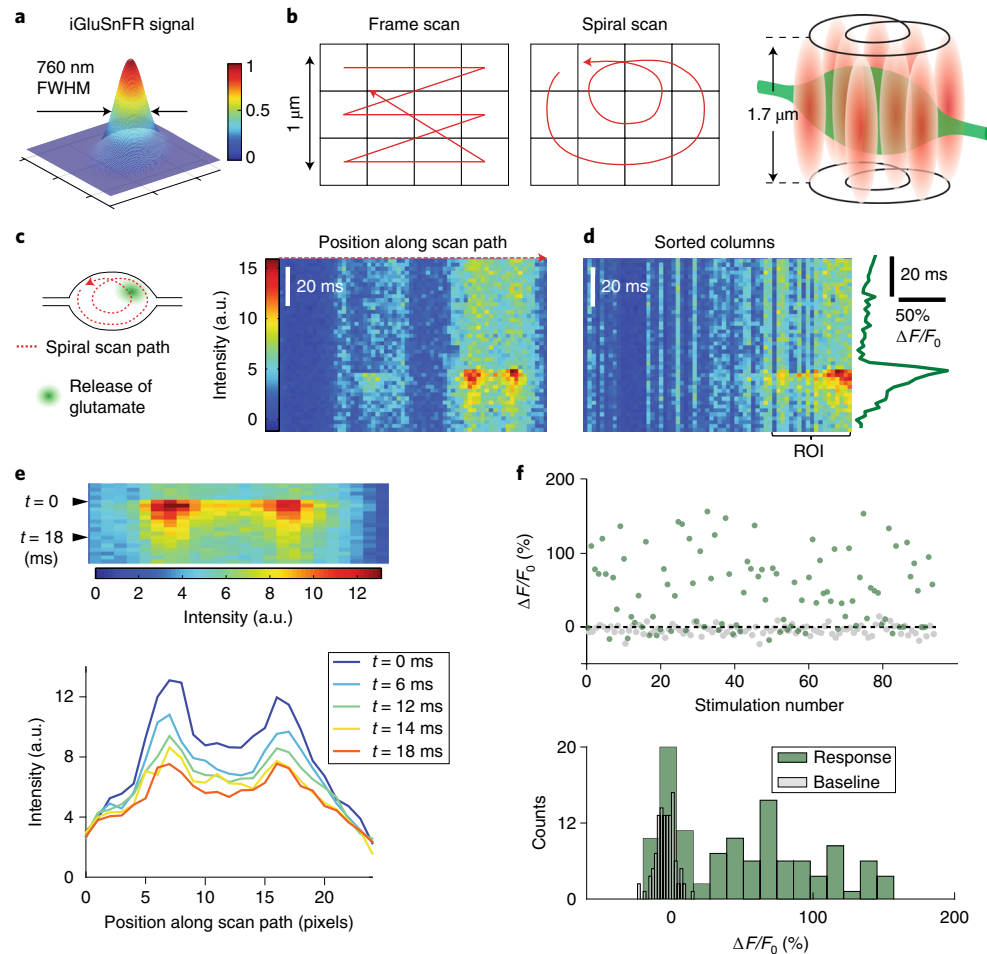


Fig. 5 | Signal extraction of GEGI transients from a single Schaffer collateral bouton in CA1. **a**, The spatial extent of iGluSnFR fluorescence transients was 760 nm, on average (FWHM, short axis of Gaussian fits). No deconvolution was applied. **b**, Sampling the surface of the bouton by traditional raster scanning requires extreme acceleration of the scan mirrors at the turning points, leading to large positional errors. Spiral scans avoid sharp direction changes (no flyback) and can, therefore, sample the entire bouton surface in 1 or 2 ms. Owing to the elongated point-spread function (PSF; 1.8 μm in the axial direction), the upper and lower surface of a bouton are sampled simultaneously. **c**, Plotting the unfolded spiral scan lines versus time (single trial). Raw fluorescence intensity is coded in pseudocolors. At $t = 58$ ms, a glutamate release event from an individual presynaptic terminal occurred and was sampled twice during every spiral scan. **d**, Only columns with $\Delta F > 1/2 \text{ max}(\Delta F)$ were analyzed (ROI). Green trace: extracted fluorescence transient (before bleaching correction). **e**, Top: average of ten trials (single APs) to analyze lateral spread of the signal from $t = 0$ to $t = -18$ ms. Bottom: decay of fluorescence transient (five scan lines plotted = 18 ms). Note the lack of lateral spread of the signal due to slow diffusion of membrane-anchored GEGI. **f**, Top: iGluSnFR response amplitude (green markers) of a single bouton stimulated with single APs every 10 s. Note that response amplitudes were constant over time. A time window before stimulation was analyzed to estimate imaging noise (gray markers). Bottom: The histogram of response amplitudes shows separation between failures of glutamate release (overlap with the baseline histogram) and successes.

diffusion of free glutamate out of the synaptic cleft happens in <1 ms and cannot be resolved by iGluSnFR or another GEGI. Instead, what we observe is the relatively slow unbinding of glutamate from quasi-stationary iGluSnFR molecules, explaining the lack of lateral spread of the signal.

Materials

Biological materials

Plasmids

- pCMV iGluSnFR (iGluSnFR in the mammalian expression vector can be used for expression in HEK293T cells and as a starting point for site-directed mutagenesis (SDM) to induce new mutations; Addgene plasmid no. 41732)⁹

- pET41a(+) (bacterial expression vector used to express GEGI variants in *E. coli*; Novagen, Merck, cat. no. 70556-3)
- pET30b (bacterial expression vector used to express GEGI variants in *E. coli*; Merck, cat. no. 69909)
- pCI syn iGluSnFR (mammalian expression vector used to express iGluSnFR in neurons (hippocampal slices); Addgene plasmid no. 106123)
- pDisplay FLIPE-600n (a vector encoding GluBP 600n for expression of glutamate-binding protein GluBP 600n in *E. coli*. Purified GluBP is used for kinetic analysis in vitro; Addgene plasmid no. 13545)⁶
- pCI syn iGlu_r (mammalian expression vector used for expression of iGlu_r in neurons; Addgene plasmid no. 106121)¹³
- pCI syn iGlu_u (mammalian expression vector used for expression of iGlu_u in neurons; Addgene plasmid no. 106122)¹³
- pCI syn tdimer2 (a gift of R. Y. Tsien, University of California, San Diego²⁹, mammalian expression vector used for expression of dimeric red fluorescent protein in neurons)
- pRSET FLIPE 600n (ECFP-ybeJ-Venus)

Testing in cell lines

- HEK293T cells (Merck, cat. no. 85120602) **! CAUTION** The cell lines used in your research should be regularly checked to ensure that they are authentic and are not infected with mycoplasma.

Slice culture and recording

- Slice cultures from rodent hippocampus³⁰ **! CAUTION** Any experiments involving live rats must conform to relevant national and institutional regulations. In our case, organ explant procedures were approved by the veterinarian of the University Medical Center Hamburg-Eppendorf, Germany.

Reagents

Cloning and molecular biology

- Restriction enzymes: BglII, NotI (NEB, cat. nos. R0144 and R0189)
- T4 DNA ligase (NEB, cat. no. M0202)
- QuikChange XL Site-Directed Mutagenesis Kit (Agilent Technologies, cat. no. 200516)
- NucleoSpin Plasmid Kit (Machery-Nagel, cat. no. 740588)
- HiSpeed Plasmid Midi Kit (Qiagen, cat. no. 12643)
- LB medium (powder; Lennox; Fisher BioReagents, cat. no. BP1427)
- LB agar (granulated; Lennox; Fisher BioReagents, cat. no. BP9745)
- Kanamycin sulfate (Fisher BioReagents, cat. no. BP906) **! CAUTION** Kanamycin sulfate is toxic. Wear protective gloves, clothing, and eye protection. Wash your hands thoroughly after handling.
- PureLink HiPure Plasmid Maxiprep Kit (Life Technologies, cat. no. K210006)

General reagents

- HEPES (sodium salt; Fisher Scientific, cat. no. BP310-1)
- Imidazole
- Sodium chloride (NaCl; Sigma-Aldrich, cat. no. S7653)
- MgCl₂ solution (1 M; Invitrogen cat. no. AM9530G)
- Sodium hydroxide (NaOH; Merck, cat. no. S8045) **! CAUTION** Sodium hydroxide is dangerous. It is corrosive to metals and causes severe skin burns and eye damage. Wear protective gloves, clothing, and eye protection. Wash your hands thoroughly after handling it.
- D(+)-Glucose (Merck, cat. no. D9434)
- Potassium chloride (KCl; Sigma-Aldrich, cat. no. P9333)
- NaH₂PO₄ (Merck, cat. no. S0751)
- Hydrogen chloride (HCl; Merck, cat. no. 109057) **! CAUTION** Hydrogen chloride is dangerous. It is corrosive to metals and causes severe skin burns and eye damage. Wear protective gloves, clothing, and eye protection. Wash your hands thoroughly after handling it.

Protein expression and purification

- Pierce protease inhibitor tablets (EDTA-free; Thermo Fisher Scientific, cat. no. A32965) **! CAUTION** Pierce protease inhibitor tablets are dangerous and cause severe skin burns and eye damage. Wear protective gloves, clothing, and eye protection. Wash your hands thoroughly after handling them.

- HisTrap high-performance column (GE Healthcare, cat. no. 17524801) ▲ **CRITICAL** EDTA-free inhibitor is critical to ensuring binding of the His-tagged protein to the HisTrap high-performance column.
- SnakeSkin dialysis tubing (3.5K MWCO; 22 mm; Thermo Fisher Scientific, cat. no. 68035)
- Coomassie blue dye
- IPTG (isopropyl- β -D-thiogalactoside)

Glutamate, aspartate, and serine titration

- L-Glutamic acid (Merck, cat. no. G1251)
- L-Aspartic acid (Merck, cat. no. A8949)
- L-Serine (Merck, cat. no. S4500)
- DMEM (high glucose, GlutaMAX supplement, pyruvate; Gibco; Thermo Fisher Scientific, cat. no. 31966047)
- MEM non-essential amino acid solution (NEAA; 100 \times ; Gibco; Thermo Fisher Scientific, cat. no. 11140035)
- FBS (qualified, heat-inactivated, EU-approved, South American origin; Gibco; Thermo Fisher Scientific, cat. no. 10500056)
- Penicillin–streptomycin (10,000 U/mL; Gibco; Thermo Fisher Scientific, cat. no. 15140122)
! **CAUTION** Penicillin–streptomycin causes skin irritation and eye irritation, and may cause an allergic skin reaction and respiratory irritation. Wear protective gloves, clothing, and eye protection. Wash your hands thoroughly after handling it.
- Lipofectamine 2000 transfection reagent (Thermo Fisher Scientific, cat. no. 11668027)

Slice culture and recording

- MEM (Sigma-Aldrich, cat. no. M7278)
- Heat-inactivated horse serum (Gibco, cat. no. 16050-122)
- L-Glutamine (200 mM; Gibco, cat. no. 25030-024)
- L-Ascorbic acid (Sigma-Aldrich, cat. no. A5960)
- Insulin (1 mg/mL; Sigma-Aldrich, cat. no. I1882)
- HEPES (Sigma-Aldrich, cat. no. H4034)
- K-gluconate (Sigma-Aldrich, cat. no. G4500)
- EGTA (Sigma-Aldrich, cat. no. E0396)
- Na₂-ATP (Sigma-Aldrich, cat. no. A3377)
- Na-GTP (Sigma-Aldrich, cat. no. G8877)
- Na₂-phosphocreatine (Sigma-Aldrich, cat. no. P7936)
- NaHCO₃ (Sigma-Aldrich, cat. no. S5761)
- NaH₂PO₄ (Sigma-Aldrich, cat. no. S5011)
- Potassium chloride (Sigma-Aldrich, cat. no. S5886)
- KCl (1 M; Fluka, cat. no. 60121)
- MgSO₄ (1 M; Fluka, cat. no. 63126)
- MgCl₂ (1 M; Fluka, cat. no. 63020)
- CaCl₂ (1 M; Fluka, cat. no. 21114)
- D-Glucose (Fluka, cat. no. 49152)
- Cl₃Fe (Fluka, cat. no. 10695862)
- Carbogen (gas mixture, 95% O₂, 5% CO₂)
- Silver chloride (AgCl)
- Alexa Fluor 594 hydrazide, sodium salt (ThermoFisher, cat. no. A10438)

Equipment

- Electro-optical modulator (EOM; Conoptics, model no. 350-80 NA)
- 3 \times Telescope (Thorlabs, cat. no. GBE03-B)
- 5-mm Scan mirrors (Cambridge Technology, model no. 6215H)
- IR mirror (Semrock, cat. no. FF705-Di01-25x36)
- Water immersion objective (60 \times , numerical aperture (NA) = 1.0; Olympus, model no. LUMPLFLN 60XW)
- Oil-immersion condenser (NA = 1.4; Olympus, model U-AAC)
- In-line heater (Warner Instruments, model SF-28)
- Photomultiplier tubes (Hamamatsu, model no. H7422P-40SEL)
- 560 DXCR dichroic mirrors and 525/50 and 607/70 emission filters (Chroma Technology)

- Short-pass filters (Chroma, model no. ET700SP-2P)
- Ti:sapphire laser system with dispersion compensation (MaiTai DeepSee; Spectra Physics)
- Stereo microscope (Leica, model no. Z6 APO)
- Fluorescent microbeads (0.17- μm diameter, ThermoFisher)
- Shutter (Uniblitz, model no. NS45B)
- Amplifier (Molecular Devices, model no. MultiClamp 700B)
- Micromanipulator (Sutter Instruments, model no. MP-285)
- Motorized stage (Danaher Motion, model no. 40-40)
- Data acquisition boards (National Instruments, PCI-6110, PCIe-6321, PCIe-6353)
- Hamilton syringe (250 μL)

Testing in cell lines

- Glass-bottom plates (Sensoplate, 24 well, PS, F-bottom, black, lid, sterile, single packed; Greiner Bio One, cat. no. 662892)

Equipment for protein expression/purification

- Sonicator for lysing *E. coli* (VibraCell; Sonics & Materials)
- ÄKTA purifier or explorer (GE Healthcare)

Equipment for biophysical characterization

- Fluorescence spectrometer with magnetic stirring function (Horiba Scientific, model no. Fluorolog-3)
- Hellma fluorescence cuvettes (ultra micro; Merck, cat. no. Z802336-1EA)
- Hellma fluorescence cuvette QS (3,500 μL ; Merck, cat. no. Z600172-1EA)
- Aladdin syringe pump (World Precision Instruments, cat. no. AL-1000)
- SGE syringe (250 μL , barrel inner diameter = 2.30 mm; Trajan Scientific and Medical, cat. no. P/N 006230)
- KinetAsyst dual-mixing stopped-flow system (equipped with two circulating water baths for temperature control and a long-pass filter >530 nm. The equipment should be set up in a dark lab with red-light illumination and temperature control (20 $^{\circ}\text{C}$); TgK Scientific, cat. no. SF-61DX2)

Equipment for imaging in cell lines

- Inverted spinning-disk confocal fluorescence microscope (Marianas, model no. 3i)

Electrophysiology equipment

- LED light source for epifluorescence (CoolLED, model no. pE-4000)
- IR Dodt contrast system (Luigs & Neumann)
- Patch-clamp amplifier (Axon Instruments, model no. MultiClamp 700B)
- Microelectrode manipulator (Sutter Instrument, model no. MP-285)
- Micropipettes for whole-cell recording (borosilicate glass with filament, 1.5-mm o.d.)

Electroporation equipment

- Upright microscope (Olympus, model no. BX61WI) with a motorized stage (Luigs & Neumann, model no. V240), CCD camera and IR-DIC (IR differential interference contrast), or Dodt contrast (Luigs & Neumann, cat. no. 200-100 200 0155) **▲ CRITICAL** The electroporation microscope should be situated close to the tissue culture hood (in the same room) to prevent contamination. We built a laminar flow cabinet with a HEPA filter unit around the electroporation setup. The microscope must be mechanically isolated from the vibrations generated by the fan in the filter box; we use an active anti-vibration table.
- 20 \times Water immersion objective (Zeiss Achroplan)
- 4 \times Zoom lens system (0.5–2.0 \times magnification range)
- Vibration isolation table (Table Stable, model no. TS-150)
- Electroporation system with HL-U model pipette holder (Molecular Devices, model no. Axoporation 800A)
- Plastic syringe body (1 mL, Thermo Scientific, cat. no. S75101) as a disposable mouthpiece, connected through a Luer one-way stopcock (Fisher Scientific, cat. no. NC1250140) and thin silicone tubing to the electrode holder (Axon Instruments, model no. 1-HL-U)
- Headphones and speakers
- Microscope chamber made of a custom glass microscope slide (70 \times 100 \times 1 mm) onto which a Teflon ring (i.d.: \sim 35 mm, height: 2 mm) is fixed with silicone aquarium sealant (Dohse Aquaristik)
- Motorized micromanipulators (Luigs & Neumann)
- Silver wire (diameter: \sim 0.25 mm)

- C-shaped gold wire
- Forceps (Fine Science Tools, cat. no. 11002-16)
- Hot-bead sterilizer (Fine Science Tools, cat. no. 18000-45)
- Incubator with rapid humidity recovery and copper chamber (37 °C; 5% CO₂; Thermo Scientific, model no. Heracell 150i/160i)
- Micropipette puller (Narishige, model no. PC-10)
- Thin-walled borosilicate glass capillaries (WPI, cat. no. TW150F-3)
- Tissue culture dishes (60 mm, sterile; Sarstedt, cat. no. 83.1801)
- Ultrafree centrifugal filter units (Millipore, cat. no. UFC30GV0S)
- Micro-osmometer (Fiske, model no. 210)

Software

- ImageJ2 (<https://imagej.net/ImageJ2>)
- GraphPad Prism v.7 (<https://www.graphpad.com/>)
- ScanImage 3.8 (ref. ³¹; <https://vidriotechnologies.com/>)
- Ephus³² (<https://www.janelia.org/open-science/ephus>)
- violinplot.m (Bastian Bechtold; <https://github.com/bastibe/Violinplot-Matlab/blob/master/violinplot.m>)
- Kinetic Studio (<https://www.hi-techsci.com/instruments/kinetic-studio/>)

Reagent setup

Resuspension buffer for protein purification

Resuspension buffer is 50 mM HEPES-Na⁺, 200 mM NaCl, pH 7.5, filtered (0.2-µm pore size). Store at 4 °C for up to 2 weeks.

Elution buffer for protein purification

Elution buffer is 50 mM HEPES-Na⁺, 200 mM NaCl, and 500 mM imidazole, pH 7.5, filtered (0.2-µm pore size). Stored at 4 °C for up to 2 weeks.

Storage buffer for protein purification

Storage buffer is 50 mM HEPES-Na⁺, 100 mM NaCl, pH 7.5; store at 4 °C for up to 2 weeks.

Assay buffer for biophysical characterization

Assay buffer is 50 mM HEPES-Na⁺, 100 mM NaCl, and 2 mM MgCl₂, pH 7.5; store at 4 °C for up to 2 weeks.

Association buffers for biophysical characterization

- 1 µM GEGI in assay buffer; store at 4 °C for up to 1 d.
- 0.1–10× K_d L-Glutamic acid in assay buffer; store at 4 °C for up to 1 d. **▲ CRITICAL** To measure the full range of response in dependence of the glutamate concentration, the glutamate concentration mixed with the GEGI must be distributed around the K_d.

Dissociation buffers for biophysical characterization

- 2 mM GluBP 600n in assay buffer; store at 4 °C for up to 1 d.
- 1 µM GEGI in assay buffer; store at 4 °C for up to 1 d.
- 1 µM GEGI in assay buffer with saturating glutamate (10× K_d); store at 4 °C for up to 1 d.

Complete DMEM

Complete DMEM is DMEM, 1× NEAA, 10% (vol/vol) FBS, and 100 U/mL penicillin–streptomycin; store at 4 °C for up to 2 months.

HEK293T cell imaging buffer

HEK293T cell imaging buffer is 20 mM HEPES-Na⁺, 145 mM NaCl, 10 mM glucose, 5 mM KCl, 1 mM MgCl₂, and 1 mM NaH₂PO₄, pH 7.4; store at 4 °C for up to 6 months.

Slice culture medium

Slice culture medium is 394 mL of MEM, 20% (vol/vol) heat-inactivated horse serum, 1 mM L-glutamine, 0.01 mg/mL insulin, 14.5 mM NaCl, 2 mM MgSO₄, 1.44 mM CaCl₂, 0.00125% ascorbic

acid, and 13 mM D-glucose. The medium must be sterile-filtered (0.2- μ m pore size); store at 4 °C for up to 4 weeks.

Slice culture transduction solution

Slice culture transduction solution is 10 mM HEPES, 145 mM NaCl, 25 mM D-glucose, 2.5 mM KCl, 1 mM MgCl₂, and 2 mM CaCl₂. Measure the pH using a pH meter and adjust the pH to 7.4 by adding NaOH or HCl. Measure the osmolality with a micro-osmometer and ensure that the osmolality is between 310 and 320 mOsm/kg. If the osmolality is out of range, a mistake was made during solution preparation. The solution must be sterile-filtered (0.2- μ m pore size); store at 4 °C for up to 6 months and pre-warm the solution to 37 °C before use.

Artificial cerebrospinal fluid (ACSF) for neuronal imaging

ACSF is 25 mM NaHCO₃, 1.25 mM NaH₂PO₄, 127 mM NaCl, 25 mM D-glucose, 2.5 mM KCl, 2 mM CaCl₂, and 1 mM MgCl₂, pH adjusted to 7.4. ACSF must be saturated with 95% O₂ and 5% CO₂. Osmolality should be between 310 and 320 mOsm/kg. Store for a maximum of 1 week at 4 °C. Bubble with carbogen (95% O₂, 5% CO₂) during warm up to prevent Ca²⁺ precipitation. Maintain the perfusion reservoir at 34 °C to prevent bubble formation in the recording chamber.

K-gluconate-based intracellular solution

K-gluconate-based intracellular solution is 10 mM HEPES, 135 mM K-gluconate, 0.2 mM EGTA, 4 mM MgCl₂, 4 mM Na₂-ATP, 0.4 mM Na-GTP, 10 mM Na₂-phosphocreatine, and 3 mM L-ascorbic acid, pH adjusted to 7.2 with KOH. Osmolality should be between 290 and 300 mOsm/kg. The solution must be sterile-filtered (0.2- μ m pore size). Store at -20 °C for a maximum of 12 months. Aliquots in Eppendorf tubes can be stored at -80 °C for a maximum of 6 months. Store on ice during the experiment to slow ATP hydrolysis.

Equipment setup

Equipment for functional imaging in tissue

We built a two-photon microscope based on an Olympus BX51WI microscope with a pE-4000 LED light source for epifluorescence and IR Dodt contrast. A Ti:sapphire laser system with dispersion compensation was coupled in through an EOM, a 3 \times telescope, 5-mm scan mirrors, a compound scan lens ($f = 50 \text{ mm}^{33}$), a dual-camera port with an IR mirror, and a water immersion objective. Red and green fluorescence was detected through the objective and the oil-immersion condenser using two pairs of photomultiplier tubes. 560 DXCR dichroic mirrors and 525/50 and 607/70 emission filters were used to separate green and red fluorescence. Excitation light was blocked by short-pass filters. During epifluorescence illumination, substage PMTs were protected by an NS45B shutter. For electrical stimulation of individual neurons, we mounted the headstage of a MultiClamp 700B amplifier on an MP-285 micromanipulator on a motorized stage that also moved the perfusion chamber (quartz glass bottom). Temperature was controlled by Peltier heating of the oil-immersion condenser and in-line heating of the ACSF. The setup was controlled by MATLAB software (ScanImage³¹ and Ephus³²) via data acquisition boards. At the start of a trial, electrophysiology and image acquisition were synchronized by a hardware trigger (transistor-transistor logic (TTL) pulse). During a trial (2 s, typically), laser power was regulated via an EOM and restricted to the periods of expected glutamate release (20- to 80-ms window, depending on GEGI kinetics) to minimize bleaching. **▲ CRITICAL** To minimize bleaching by excessive excitation, the microscope must be designed to detect emitted photons very efficiently. Using only the objective for fluorescence detection is not sufficient to achieve single-vesicle sensitivity. Condenser detection (oil immersion, 1.4 NA, large field of view) is essential to the success of single-synapse experiments with many trials. Replace aging PMTs that show excessive dark counts. **▲ CRITICAL** The oil-immersion condenser must be permanently heated (day and night) if a recording temperature above room temperature (20 °C) is desired. This can be achieved with flexible heating pads or Peltier elements. As the thermal mass of the condenser is very large, constant-current heating is sufficient, provided that the temperature of the ACSF is additionally regulated by a feedback control circuit (in-line heater). A climate chamber would be an attractive solution but is not compatible with direct-mounted PMTs. **▲ CRITICAL** If a galvanometric scanning system is used, the microscope software must support arbitrary line scans or spiral scans³⁴. The code for arbitrary line scans that we developed for our original study is now incorporated

into the ScanImage software (v.2016 and later). ScanImage is developed and supported by Vidrio Technologies as an open-source research resource. A resonant scanning system may be sufficiently fast in frame mode if extreme zoom-in (few scan lines) can be realized.

Procedure

Generation of GEGIs ● Timing 1 week;5-h hands-on time

▲ **CRITICAL** We have made a number of GEGI-encoding plasmids available via Addgene (see the Reagents section). Follow Steps 1–42 in order to design GEGIs with tailored biophysical parameters.

- 1 Analyze protein 3D structures of the 99% homolog of GltI of *Shigella flexneri* (PDB 2VHA) and the literature^{35,36} to assign critical residues involved in glutamate binding. Substitute essential residues with amino acids with similar physical properties. Avoid radical changes in amino acid size or charge, as this will frequently result in misfolded or otherwise nonfunctional proteins.
- 2 Subclone the *iGluSnFR* gene from a mammalian expression vector into a bacterial expression vector (pET41a) using restriction digestion of BglII and NotI and ligation (T4 DNA ligase), following the manufacturer's protocol.
! **CAUTION** Subcloning requires DNA to be analyzed by agarose gels. This requires the use of DNA-intercalating fluorescent dyes (e.g., ethidium bromide or Sybr green) that are highly toxic mutagens and should be handled with care. DNA imaging systems are based on UV lamps, so appropriate personal protective equipment should be used.
- 3 Insert point mutations using the QuikChange XL Site-Directed Mutagenesis Kit and following the manufacturer's instructions; confirm new variants by DNA sequencing.
- 4 Subclone the *gltI* gene encoding GluBP 600n from pRSET FLIPE 600n (ECFP-ybeJ-Venus) into pET30b (His-fusion expression vector) at the BglII and NotI restriction sites.

Expression and purification of new GEGIs ● Timing 3 d; 10-h hands-on time

- 5 Transform 1 μL of iGluSnFR variants or GluBP 600n plasmid DNA into 50 μL of *E. coli* BL21 (DE3) gold chemically competent cells.
- 6 Pick one colony and grow it overnight in 10 mL of LB medium supplemented with 100 μg/mL kanamycin at 37 °C on an orbital shaker set to 180 r.p.m. (pre-culture).
- 7 Inoculate 1 L of LB medium containing 100 μg/mL kanamycin with whole pre-culture and incubate at 37 °C on an orbital shaker set to 180 r.p.m. until the OD₆₀₀ value reaches 0.6–0.8.
- 8 Cool the cells to 20 °C.
- 9 Induce protein expression with 0.5 mM IPTG and incubate at 20 °C and 180 r.p.m. on an orbital shaker overnight.
▲ **CRITICAL STEP** Best protein yields are obtained when inducing expression during the exponential phase of growth (OD₆₀₀ 0.6–0.8), overnight at 18–20 °C.
- 10 Harvest the cells by centrifugation at 3,000g for 15 min at room temperature, resuspend the cells in 40 mL of resuspension buffer supplemented with Pierce protease inhibitor (prepared according to the manufacturer's instructions), and lyse via sonication on ice for 2 min (2 s 'on' and 8 s 'off').
! **CAUTION** Wear ear protection equipment during sonication.
▲ **CRITICAL STEP** Sonication produces heat and may result in the degradation of your protein of interest. Performing sonication on ice and in the presence of protease inhibitors will markedly limit this phenomenon.
- 11 Remove the cell debris by ultracentrifugation at 100,000g for 45 min at 4 °C.
▲ **CRITICAL** After cell lysis, all steps are performed at 4 °C, when possible, to avoid protein digestion by cellular proteases (Steps 12–14).
- 12 Load the supernatant on an equilibrated HisTrap high-performance column (nickel affinity resin) mounted on an ÄKTA purification system (flow rate = 4 mL/min) and wash with 40 mL of resuspension buffer.
- 13 Elute the protein with ten column volumes of a linear gradient of resuspension and elution buffer (0–0.5 M imidazole) and collect in 2-mL fractions. Analyze the purified protein by SDS–PAGE and stain the gel with Coomassie blue.
- 14 Pool the fractions of interest and dialyze overnight at 4 °C in a SnakeSkin Dialysis Tubing (3.5 kDa) against 4 L of storage buffer.
▲ **CRITICAL STEP** It is essential to perform dialysis to remove the imidazole from your buffer. Otherwise, protein precipitation will occur upon defrosting (from Step 15). The dialysis MWCO used can be higher than 3.5 kDa, as long as it is <15 kDa.

- 15 Store purified protein in 1-mL fractions in a $-80\text{ }^{\circ}\text{C}$ freezer.
■ PAUSE POINT The purified protein can be stored at $-80\text{ }^{\circ}\text{C}$ for up to 3 years.

Determination of the dynamic range ● Timing 1 h

- 16 Prepare 50–100 nM iGluSnFR proteins in assay buffer, add to a Hellma microcuvette (50 μL), and place the cuvette into a fluorescence spectrometer pre-equilibrated to $20\text{ }^{\circ}\text{C}$.
- 17 Record the fluorescence emission spectrum ($\lambda_{\text{ex}} = 492\text{ nm}$ and $\lambda_{\text{em}} = 497\text{--}550\text{ nm}$) ($F_{\text{-glu}}$).
- 18 Add 10 mM glutamate solution to the microcuvette, mix well, and record the fluorescence emission spectrum ($\lambda_{\text{ex}} = 492\text{ nm}$ and $\lambda_{\text{em}} = 497\text{--}550\text{ nm}$) ($F_{\text{+glu}}$).
- 19 To analyze the data, take the maximal emission ($\sim 514\text{ nm}$) of each measurement and calculate the fluorescence dynamic range ($(F_{\text{+glu}} - F_{\text{-glu}})/F_{\text{-glu}}$).
- 20 Repeat Steps 16–19 twice in order to generate three independent replicates.
▲ CRITICAL STEP If the fluorescence dynamic range is <2 , the fluorescence change upon glutamate binding is too low for imaging in hippocampal slices. In that case, try using higher concentrations of glutamate. If the fluorescence dynamic range does not improve, return to Step 1 and select another mutation.

Determination of K_{d} and specificity ● Timing 2 h per ligand

- 21 Prepare 50–100 nM GEGI in 3-mL of assay buffer in a 3,500- μL Hellma quartz cuvette (QS).
- 22 Add a magnetic stir bar and place the cuvette into a spectrofluorometer.
▲ CRITICAL STEP Make sure that the stir bar is moving rigorously.
- 23 Fill a 250- μL Hamilton syringe with assay buffer containing the appropriate ligand: L-glutamate ($10\times K_{\text{d}}$ 10–50 mM), L-aspartate ($10\times K_{\text{d}}$ 10–50 mM), or L-serine ($10\times K_{\text{d}}$ 10–50 mM).
▲ CRITICAL STEP Make sure that there are no air bubbles in the syringe nor in the tubing.
- 24 Install the syringe in an Aladdin syringe pump, set the flow rate to 10 $\mu\text{L}/\text{min}$, and place the tubing outlet carefully into the microcuvette.
- 25 Simultaneously start the recording of the fluorescence emission over time ($\lambda_{\text{ex}} = 492\text{ nm}$ and $\lambda_{\text{em}} = 514\text{ nm}$) and the syringe pump.
- 26 To analyze the data, use time information to calculate the ligand concentration in the cuvette at each given time point. Correct the fluorescence emission for dilution/photobleaching and normalize it. Plot the corrected and normalized fluorescence against the ligand concentration and fit with a Hill equation for specific binding (GraphPad Prism v.7) to obtain affinity for glutamate (K_{d}) and cooperativity of binding (n).
- 27 Repeat Steps 21–26 twice in order to generate at least three independent experiments.

Measurement of kinetics ● Timing 5 h; 4 h for association and 1 h for dissociation

- ▲ CRITICAL** Temperature control is essential for all kinetic measurements. Furthermore, washing the instrument thoroughly after changing the ligand concentration is critical. To correctly analyze the data, baselines and maximum fluorescence intensity lines should be recorded as described below. Always average at least five records (“shots”) for each measurement to obtain a representative trace.
- 28 *Association (Steps 28–32)*. Mix 1 μM GEGI in assay buffer with the maximal glutamate concentration in assay buffer ($10\times K_{\text{d}}$, as determined in Step 27). Set the fluorescence level after mixing to reach 80% detector saturation by adjusting the gain on the PMT (reference of 1 for normalization). This step will prevent detector overload in future experiments.
 - 29 Mix assay buffer with assay buffer (identical solutions) and record the baseline (reference of 0 for normalization). Note that due to the dark noise of the PMT, the reading may not be zero.
 - 30 Mix 1 μM GEGI in assay buffer with assay buffer. This measurement should result in a straight line and shows the basal fluorescence without a ligand bound.
▲ CRITICAL STEP Steps 28–30 must be performed before starting any association kinetic measurement of a GEGI. This ensures that the instrument is calibrated for maximum/minimum fluorescence detection levels and prevents detector damage.
 - 31 *Glutamate-dependent association kinetics*. Mix 1 μM iGluSnFR variant in assay buffer with increasing glutamate concentrations in assay buffer ($0.1\text{--}10\times K_{\text{d}}$). Record and average five measurements for each glutamate concentration.
▲ CRITICAL STEP You may have to perform measurements of different time scales to have enough data points for an accurate exponential fitting. Make sure that you use about ten different glutamate

- concentrations to measure the fluorescence increase with increasing glutamate and also the saturation, indicated by reaching a maximum fluorescence intensity and on-rate.
- 32 To analyze the data, normalize the recorded time traces to the PMT baseline and the maximal fluorescence level. Fit the time traces with mono- or biexponential decays (Kinetic Studio or GraphPad Prism v.7). Plot the obtained observed rate constants against the glutamate concentration.
 - 33 *Dissociation (Steps 33–37)*. Mix 1 μM GEGI in glutamate saturating assay buffer ($10\times K_d$, as determined in Step 27) with the same buffer. Set the fluorescence level after mixing to reach 80% detector saturation by adjusting the gain on the PMT (reference of 1 for normalization). This step will prevent detector overload in future experiments.
 - 34 Perform Step 29 to obtain the reference for 0.
 - 35 Perform Step 30 to obtain the basal fluorescence level.

▲ CRITICAL STEP Steps 34 and 35 must be performed before starting any dissociation kinetic measurement of a GEGI. This ensures that the instrument is calibrated for maximum/minimum fluorescence detection levels and prevents detector damage.
 - 36 *Dissociation kinetics*. Mix 1 μM GEGI in assay buffer with saturating glutamate concentration ($10\times K_d$) with 2 mM GluBP 600n in assay buffer. Higher concentrations of GluBP 600n are not advisable, as precipitation might occur. Record and average five measurements.

▲ CRITICAL STEP You may have to perform measurements of different time scales to have enough data points for an accurate exponential fitting.
 - 37 To analyze the data, normalize the recorded time traces to the PMT baseline and the maximum fluorescence level. Then fit the time trace with mono- or biexponential decays (Kinetic Studio or GraphPad Prism v.7). Plot the obtained observed rate constants against the glutamate concentration.

Determination of fluorescence dynamic range and K_d in HEK293T cells ● Timing 2 d; 5-h hands-on time

- 38 Seed ~200,000 cells onto 24-well glass-bottom plates (SensyPlate) in complete DMEM and let them attach for 24 h in the incubator (37 °C, 5% (vol/vol) CO₂).
- 39 Transfect the cells with GEGI plasmids generated by SDM of promising mutations into the mammalian expression vector pCMV iGluSnFR, using Lipofectamine 2000 and following the manufacturer's protocol.
- 40 Examine the cells 24 h post transfection in HEK283T cell-imaging buffer at 37 °C with a confocal microscope (light source = 488 nm, using GFP settings). Check for localization at the plasma membrane.
- 41 *Glutamate titration*. Add glutamate stepwise to final concentrations between 0 and $10\times K_d$ (as determined in Step 27) and take an image of the cells before and after each addition step.

▲ CRITICAL STEP Focus drift may happen when you add glutamate. If that is the case, discard the last data point and move to a different well.
- 42 Define elliptical ROIs along the cell membrane and determine the fluorescence intensity (ImageJ). Normalize the intensity for each individual cell and average over a total number of >20 cells. Plot the relative intensity versus glutamate concentration and fit the data with Hill equation (GraphPad Prism v.7).

Cloning in neuronal expression vector ● Timing 7 d; 5-h hands-on time

- 43 Use a QuikChange XL Site-Directed Mutagenesis Kit to insert mutations of promising GEGI variants into the pCI syn iGluSnFR vector and confirm by DNA sequencing.
- 44 Prepare the plasmid for electroporation using a plasmid DNA preparation kit (e.g., PureLink HiPure Plasmid Maxiprep Kit).

Culture preparation ● Timing 15 min per brain

- 45 Prepare organotypic slice cultures (rat hippocampus) as described in ref. ³⁰.

Single-cell electroporation ● Timing 10 min plus 10–20 min per slice, depending on slice quality and number of cells to transfect

- 46 *Preparation of plasmids and DNA (Steps 46 and 47)*. Sterile-filter an aliquot (0.5 mL) of K-gluconate-based intracellular solution through a Millipore Ultrafree centrifugal unit by centrifugation at 16,000g for several seconds in a tabletop centrifuge at 4 °C.

- 47 After removal of the filter insert, add the GEGI plasmids to the desired concentration. Use 40–50 ng/μL for pCI syn iGlu_f or pCI syn iGlu_{ii} (ref.¹³). For different cell types and GEGIs, the final concentration may have to be determined empirically (range: 1–100 ng/μL).
▲ CRITICAL STEP It is important that the DNA-containing solution is not passed through the Millipore Ultrafree centrifugal filter unit.
▲ CRITICAL STEP To aid visualization of axons and boutons of transfected neurons, mix plasmid encoding for RFP (e.g., tdimer2; 20 ng/μL) with GEGI plasmid to achieve co-expression.
■ PAUSE POINT The electroporation solution containing the plasmid can be stored between electroporation sessions at –20 °C for up to 1 year.
- 48 *Electroporation (Steps 48–56)*. Coat silver wire tips and ground electrodes with AgCl by bathing them in a saturated Cl₃Fe solution for at least 30 min or overnight before first use.
- 49 Use a micropipette puller (e.g., PC-10) to pull electroporation pipettes. Pull thin-walled borosilicate capillaries to obtain a resistance of 10–15 MΩ when filled with the K-gluconate-based intracellular solution.
▲ CRITICAL STEP Ensure constant pipette resistance for reproducible expression. A too-high pipette resistance leads to low expression, whereas a too-low resistance causes extreme expression levels and toxicity.
- 50 Backfill an electroporation pipette with ~1.2 μL of plasmid mix solution (from Step 47) for each slice to be electroporated. Backfilled pipettes can be kept (in an upright position) for up to 2 h before use. Pipette 1 mL of slice culture transduction solution (37 °C) into the microscope chamber. Transfer one slice culture insert to the chamber (sterile forceps) and add slice culture transduction solution on top of the slice culture for the water immersion objective. Use a sterile 60-mm dish to cover the microscope chamber and transfer it to the microscope to proceed to single-cell electroporation.
▲ CRITICAL STEP To avoid any contamination, place forceps into the hot-bead sterilizer for ~10 s before any handling of insert.
▲ CRITICAL STEP Work on an electrophysiology microscope setup in a laminar flow box (see the ‘Equipment’ section) to prevent contamination.
- 51 Apply positive pressure to the pipette to approach a cell to electroporate. Monitor the tip resistance of the electroporation pipette by audio output of the Axoprotator 800A amplifier throughout the entire procedure. The resistance should be between 10 and 15 MΩ.
▲ CRITICAL STEP Similarly to patch-clamp recording technique, positive pressure on the electroporation pipette is maintained to keep the tip of the pipette clean while penetrating the tissue.
▲ CRITICAL STEP For a reproducible expression level of the plasmids between different electroporation sessions, ensure that the pipette resistance is constant.
- 52 Move the tip of the electroporation electrode close to a cell of interest while reducing the positive pressure.
- 53 Approach the cell without sealing the electrode with membranes from other cells in the tissue. Touch the plasma membrane, which will cause a rise in tip resistance, indicated by a rise in pitch. Immediately release the pressure and wait for the resistance to increase to 25–40 MΩ. Do not apply suction and avoid the formation of a gigaohm seal.
- 54 Apply a pulse train (e.g., voltage: –12 V, frequency: 50 Hz, pulse width: 500 μs, and train duration: 500 ms). The optimal settings may differ depending on the cell type to be electroporated.
▲ CRITICAL STEP For more reproducible expression levels of the plasmids between different cells, try to wait for the resistance to increase to a similar value before applying the pulse train.
- 55 Slowly retract the pipette and begin applying very light positive pressure once the pipette is retracted 2–4 μm away from the soma. Increase the positive pressure at more considerable distances from the electroporated cell in order to maintain the cleanliness of the pipette tip. Using the same electrode, repeat Steps 51–55 for each cell to be electroporated.
- 56 Cover the chamber with a 60-mm dish and transfer it back to the tissue culture hood. Remove all transfection medium and return the insert to the slice culture medium. Typically, 2–4 d are needed for optimal expression levels of GEGIs in hippocampal organotypic slices. However, the optimal time for a cell to express a given plasmid before starting the experiment must be determined empirically³⁷.

Stimulation of transfected neurons ● Timing 30–90 min per recording, depending on slice quality, the number of cells expressing the electroporated plasmids, and the length of the recording

- 57 Start a temperature-controlled perfusion system with ACSF and place the organotypic culture in the recording chamber. Weigh down the membrane patch with a c-shaped gold wire.
? TROUBLESHOOTING
- 58 Tune the Ti:sapphire laser to 980 nm for simultaneous excitation of tdimer2 and GEGI.
? TROUBLESHOOTING
- 59 Approach a transfected CA3 neuron with the patch pipette, switching between red epifluorescence and IR Dodt contrast (CCD camera).
? TROUBLESHOOTING
- 60 Establish a gigaohm seal and rupture the membrane patch by brief suction to establish whole-cell configuration.
▲ CRITICAL STEP Stimulate an individual transfected cell to avoid stimulation of presynaptic terminals close to the terminal under scrutiny. This will ensure that the GEGI transients originate from the imaged terminal and are not a consequence of glutamate spillover.
- 61 Move the stage to center the objective on CA1. Use two-photon excitation to search for red fluorescent axons.
? TROUBLESHOOTING

Imaging synaptic glutamate release

- 62 Scan modality and signal analysis depend on the synaptic parameter under scrutiny. To localize the fusion site, acquire fast frame scans followed by fitting with a Gaussian kernel (option A). To analyze the amplitude of glutamate transients, acquire spiral scans (option B). To extract the amplitude, define an ROI in each trial and fit an exponential decay function to the extracted time course.
 - (A) **Fusion site localization ● Timing 1 h per recording**
 - (i) Inject current pulses (2–3 ms, 1.5–3.5 nA) into the soma and acquire rapid frame scans of a single bouton (high zoom, 16 × 16 pixels, 1 ms per line).
 - (ii) Treat the raw images by a wavelet method to reduce photon shot noise³⁸ and improve SNR.
? TROUBLESHOOTING
 - (iii) Upsample the images to 128 × 128 pixels (Lanczos kernel).
 - (iv) Align the images, using a fast Fourier transform performed on the red fluorescence signal (tdimer2).
 - (v) Define a morphology mask to define a continuous area encompassing bouton and axon (pixel intensity ≥10–30% maximal intensity).
 - (vi) Calculate the relative change in GEGI fluorescence ($\Delta F/F_0$) pixel by pixel, using the mean of five baseline frames as F_0 . Calculate the relative change and average the top 3% pixel values (of the GEGI signal) within the bouton mask to obtain the peak amplitude.
 - (vii) Construct a template (2D anisotropic Gaussian kernel) from the average of five trials classified as successes. A trial is classified as success when the peak amplitude is $>2\sigma$ of the baseline frames.
 - (viii) Perform a first round of analysis by fitting the template to each single frame by adapting only the amplitude and keeping the location and shape of the kernel fixed at the template values to obtain a preliminary classification of ‘successes’ ($\Delta F/F_0 > 2\sigma$ of baseline noise) and ‘failures’ ($\Delta F/F_0 < 2\sigma$ of baseline noise).
 - (ix) Repeat the fitting procedure on all trials classified as successes (Step (viii)), allowing for variable location in order to localize the fusion site.
? TROUBLESHOOTING
 - (x) As a control, apply the same localization procedure to the failure trials and to the frame before stimulation.
? TROUBLESHOOTING
 - (B) **Amplitude extraction and failure analysis ● Timing 1 h per recording**
 - (i) Inject current pulses (2–3 ms, 1.5–3.5 nA) into the soma and acquire rapid frame scans of a single bouton (high zoom, 16 × 16 pixels, 1 ms per line).
 - (ii) If a bouton shows AP-induced fluorescence increase (green channel), switch to spiral scan mode.
? TROUBLESHOOTING

Box 1 | Bleaching of GEGI

During imaging, some GEGI molecules bleach, leading to a decrease in baseline fluorescence during each trial (Supplementary Fig. 1). This may cause problems when fitting an exponential function to the decay of the glutamate response, because at least two time constants must be taken into account. To correct individual trials from one bouton for bleaching, fit an exponential decay function to the average of several 'failure' trials. Subtract this function from each trial (failures and successes; Step 62B(viii)). Between trials, fluorescence partially recovers, indicating lateral diffusion of GEGI molecules within the axonal membrane. Some loss of GEGI fluorescence (20–40%) during the course of the experiment can be tolerated because it does not affect the glutamate-induced relative change in fluorescence ($\Delta F/F_0$; Supplementary Fig. 1). We found that manual refocusing between trials can lead to substantial bleaching of the indicator. This can be minimized by automated refocusing between trials.

- (iii) Acquire AP-induced GEGI transients at regular intervals (10 s), using 500- or 1,000-Hz sampling. Image only for the duration of the GEGI transients (~20–80 ms) to minimize laser exposure.
 - (iv) For amplitude extraction, linearize the spiral scans and display them as space–time (x–t) plots (Fig. 5c).
 - (v) To distinguish successful glutamate release events from failures, perform a statistical comparison of fluorescence fluctuations before stimulation (ΔF baseline, $n = 64$ columns/locations) and response amplitude (ΔF response, $n = 64$ columns/locations). A significant difference suggests a success; lack of significance suggests a failure. This classification is preliminary; the final failure analysis is performed after amplitude extraction (Step (xi)).
 - (vi) As there may be lateral drift between individual trials, it is necessary to assign a new ROI for each success trial. The spiral scan covering the entire bouton may hit the GEGI transient once or several times per line. Sort the pixel columns (i.e., spatial positions) according to the change in fluorescence (ΔF) in each column (Fig. 5d). In a given trial, only the columns that display a clear change in fluorescence ($\Delta F > 1/2 \max \Delta F$) are analyzed (ROI). The threshold is adjusted once according to the noise of the imaging system but should be kept constant for amplitude comparisons between different experiments.
 - (vii) In failure trials, evaluate columns/locations identical to those used in the last success trial.
 - (viii) If necessary, correct traces for GEGI bleaching (Box 1).
 - (ix) For each bouton, extract the characteristic decay time constant (τ) by fitting a mono-exponential function to the average GEGI fluorescence transient.
 - (x) Estimate the glutamate transient amplitude for each trial by fitting an exponential function to the decay of the fluorescence transient (fixed τ ; amplitude as the only free parameter).
- ? TROUBLESHOOTING**
- (xi) For each trial, determine the imaging noise (σ) from the baseline of the extracted fluorescence time course. Classify as 'success' a trial for which average $\Delta F/F_0 > 2\sigma$ above baseline imaging noise; otherwise, classify the trial as 'failure'.

Troubleshooting**Step 57**

Slices are contaminated. See ref. ³⁰ for proper slice culture handling.

Step 58

No cells express the construct. Ensure that the constructs are incorporated into the target cells by adding a fluorescent dye, such as Alexa Fluor 594, to the DNA mix (Step 47). After applying the pulse train to the target neuron (Step 54), take a fluorescence image (e.g., Leica Z6 APO) to ensure that the DNA solution and fluorescent dye were successfully electroporated. For more details for the electroporation procedure, refer to ref. ³⁷.

Step 59

Cells are dying after transfection with the constructs. Lower the expression of the GEGI, ensure that the pipette resistance (Step 49) is not <10–15 M Ω in the bath before electroporation, and/or reduce expression time. A large pipette tip diameter (low resistance) can lead to overexpression of the GEGI and cell toxicity. Cells should be imaged 2–4 d after electroporation, as longer expression of GEGIs can affect cell health.

! CAUTION Very strong promoters (cytomegalovirus (CMV)) should not be used for physiological experiments in neurons.

Step 61

The slice is drifting; focus is not stable. Lower the perfusion rate. Check that the temperatures of the ACSF and of the imaging chamber of the microscope are stable to avoid thermal expansion during the experiment.

Step 62A(ii)

The responses are very weak and barely above noise. Wait longer after electroporation for a higher expression level. If the expression levels are too low, the GEG signal from a single vesicle may be below the detection limit. The detection limit is determined by the noise level of the optical recording setup. Minimize background fluorescence, which can be caused by leaking room light, stray pump laser photons (green), or excessive dark counts in aging PMTs. Condenser detection is sensitive to the refractive index of the immersion oil and correct (Köhler) position.

Step 62A(ix)

The localization seems inaccurate. Calibrate the optical and mechanical performance of your system, using fluorescent microbeads. Imaging of microbeads (0.17- μm diameter) positioned next to a fluorescent presynaptic terminal allows quantification of the accuracy of the response localization procedure.

Step 62A(x)

In cases in which the positions of apparent ‘failures’ cluster in a second area of the bouton, exclude the bouton from further analysis, as it might be a multi-synapse bouton.

Step 62B(ii)

The success rate in finding a bouton releasing glutamate is very low. This can be due to low release probability. Check the Ca^{2+} concentration of the ACSF.

Step 62B(x)

In some trials, the baseline fluorescence may show large fluctuations caused by green fluorescent vesicles passing through the axon. Remove these trials from further analysis.

Timing

Steps 1–4, generation of GEGIs: 7 d; 5-h hands-on time

Steps 5–15, expression and purification of new GEGIs: 3 d; 10-h hands-on time

Steps 16–20, dynamic range determination: 1 h

Steps 21–27, determination of K_d and specificity: 2 h per ligand

Steps 28–32, measurement of association kinetics: 4 h per variant

Steps 33–37, measurement of dissociation kinetics: 1 h per variant

Steps 38–42, determination of fluorescence dynamic range and K_d in HEK293T cells: 2 d; 5-h hands-on time

Steps 43 and 44, subcloning into neuronal expression vector: 7 d; 5-h hands-on time

Step 45, culture preparation: 15 min per brain

Steps 46 and 47, preparation of plasmids and DNA: 10 min

Steps 48–56, single-cell electroporation: 10–20 min per slice

Steps 57–61, stimulation of transfected neurons: 30–90 min per recording, depending on slice quality, the number of cells expressing the electroporated plasmids, and the length of the recording

Step 62A(i–x), fusion site localization: 1 h per recording

Step 62B(i–xi), amplitude extraction and failure analysis: 1 h per recording

Anticipated results

Assessing the properties of neighboring boutons

Once a responding bouton is identified, several neighboring boutons along the same axon can be imaged sequentially. Neighboring boutons frequently have similar release probabilities and response amplitudes (Fig. 6a). In rare cases, however, we found dramatic differences in response amplitude

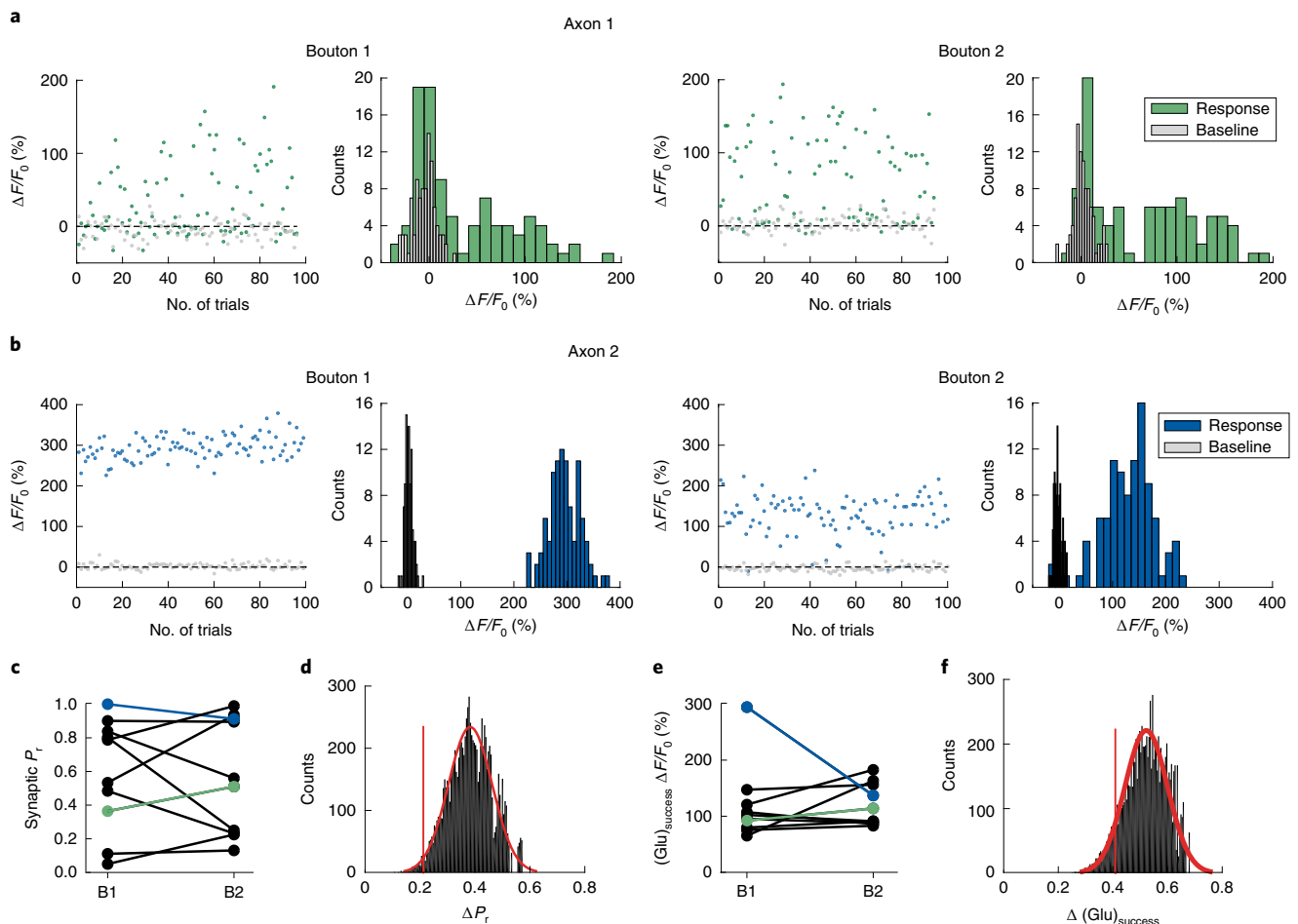


Fig. 6 | Release statistics of neighboring boutons on the same axon. **a**, Glutamate transients (green dots) and baseline fluorescence (gray dots) of two neighboring boutons located on the same axon measured in ACSF containing 2 mM Ca^{2+} and 1 mM Mg^{2+} (left panels) and their corresponding histogram counts (right panels). **b**, Glutamate transients (blue dots) and baseline fluorescence (gray dots) of two neighboring boutons located on the same axon measured in ACSF containing 2 mM Ca^{2+} and 1 mM Mg^{2+} (left panels) and their corresponding histograms (right panels) and their corresponding histogram counts (right panels). **c**, Synaptic release probability (P_r) (calculated out of ~100 trials) of individual boutons (B1) and their neighboring bouton on the same axon (B2); $n = 10$. The pair of neighboring boutons from **a** and **b** are shown in green and blue, respectively. **d**, Histogram of $\Delta P_r = |P_r, \text{BX} - P_r, \text{BY}|$. BX and BY are randomly paired from the dataset in **c**. The measured difference in P_r , $|P_r, \text{B2} - P_r, \text{B1}|$ (red vertical line), is significantly smaller than the mean ΔP_r of two boutons paired randomly from the same dataset; ($P = 0.0148$). **e**, Amplitude of the iGluSnFR signal given a success of a bouton B1 and its neighbor on the same axon (B2); $n = 10$. The pair of neighboring boutons from **a** and **b** are shown in green and blue, respectively. **f**, Histogram of the difference between the average $\Delta F/F_0$ of successes only of two random boutons. The measured difference of the average $\Delta F/F_0$ of successes from two neighboring boutons (red vertical line) is not significantly different from the mean difference between randomly selected boutons.

between neighboring boutons (Fig. 6b). To test whether boutons on the same axon are functionally similar, we generated random pairs by drawing from our entire set of characterized boutons. The differences between randomly selected boutons are normally distributed (black bars in Fig. 6d). The actual difference between neighboring boutons (Fig. 6c; red line in Fig. 6d) is at the low end of the distribution, indicating that neighboring boutons tended to have similar release probabilities. A similar result, however nonsignificant, was found when response amplitudes were analyzed (Fig. 6e,f).

Application of fast GEGs

Although iGluSnFR has an excellent SNR, it is too slow to resolve vesicle fusion events during high-frequency transmission³⁹. The recently developed ultrafast GEGs iGlu_u and iGlu_f¹³ resolve individual responses during 100-Hz trains, albeit with slightly lower SNR, as shorter transients correspond to fewer photons collected (Fig. 7a). For these experiments, scan speed was increased to 1 kHz, and a high Ca^{2+} solution was used to increase release probability. Under these conditions, individual

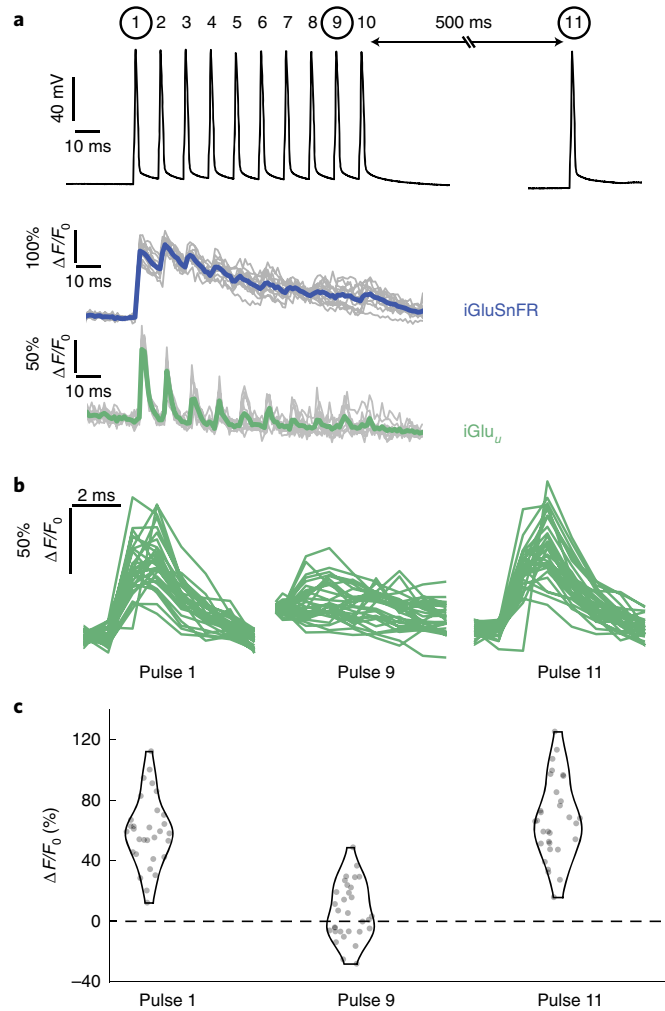


Fig. 7 | Resolving high-frequency transmission with ultrafast GEGI, iGlu_u. **a**, The presynaptic neuron was driven to spike at 100 Hz (ten APs). After a pause of 0.5 s, one more AP was triggered to quantify recovery from depression. iGluSnFR signals (blue) or iGlu_u signals (green) were recorded at single Schaffer collateral boutons (only during the 100-Hz train) in the stratum radiatum. Recordings were performed in 4 mM Ca²⁺ and 1 mM Mg²⁺ to ensure a very high release probability. Note the summation and saturation of iGluSnFR (but not iGlu_u) during the high-frequency train. **b**, iGlu_u responses to the first AP of the 100-Hz train, to the ninth AP of the train, and to the recovery pulse. To minimize bleaching, the bouton was imaged (spiral scans) only during pulses 1, 9, and 11. Note the frequent failures in response to pulse 9. **c**, Extracted single-trial amplitudes reveal strong depression and full recovery of this bouton. Failures of glutamate release can be seen in response to pulse 9. Note the large amplitude of initial responses compared to depressed responses. Plots were generated with violinplot.m.

boutons typically had a release probability of 1 on the first AP, which rapidly dropped to ~0.2 toward the end of the 100-Hz train. After a brief recovery period (0.5 s), most boutons could restore their initial high-release probability (Fig. 7b,c). Interestingly, the depression also affected the amplitude of individual successes, suggesting a switch from multivesicular release (MVR) to univesicular release during high-frequency activity^{1,40}. Alternatively, a switch from full fusion to partial fusion of synaptic vesicles⁴¹ could explain this observation. Responses from an iGluSnFR-expressing bouton during high-frequency stimulation are shown for comparison (blue traces, Fig. 7a). Summation of 100-Hz release events drives this slow GEGI toward saturation, making it impossible to disentangle single-pulse responses by deconvolution. As saline with a high calcium concentration (4 mM) was used in these experiments, the prevalence of MVR under more physiological conditions remains to be investigated. In this context, an important advantage of GEGI measurements, as compared with those for genetically encoded Ca²⁺ indicators (GECIs)⁴², is their independence from extracellular [Ca²⁺], allowing investigation of the impact of changes in [Ca²⁺]_e on presynaptic function⁴³. In summary,

ultrafast GEGIs allow direct visualization of short-term plasticity at individual synapses and may help unravel the underlying biophysical mechanisms.

Reporting Summary

Further information on research design is available in the Nature Research Reporting Summary linked to this article.

Data availability

The data that support the findings of this study are available from the corresponding author on request.

References

1. Pulido, C. & Marty, A. Quantal fluctuations in central mammalian synapses: functional role of vesicular docking sites. *Physiol. Rev.* **97**, 1403–1430 (2017).
2. Choquet, D. & Triller, A. The dynamic synapse. *Neuron* **80**, 691–703 (2013).
3. Namiki, S., Sakamoto, H., Iinuma, S., Iino, M. & Hirose, K. Optical glutamate sensor for spatiotemporal analysis of synaptic transmission. *Eur. J. Neurosci.* **25**, 2249–2259 (2007).
4. Okubo, Y. et al. Imaging extrasynaptic glutamate dynamics in the brain. *Proc. Natl. Acad. Sci. USA* **107**, 6526–6531 (2010).
5. Brun, M. A. et al. A semisynthetic fluorescent sensor protein for glutamate. *J. Am. Chem. Soc.* **134**, 7676–7678 (2012).
6. Okumoto, S. et al. Detection of glutamate release from neurons by genetically encoded surface-displayed FRET nanosensors. *Proc. Natl. Acad. Sci. USA* **102**, 8740–8745 (2005).
7. Tsien, R. Y. Building and breeding molecules to spy on cells and tumors. *FEBS Lett.* **579**, 927–932 (2005).
8. Hires, S. A., Zhu, Y. & Tsien, R. Y. Optical measurement of synaptic glutamate spillover and reuptake by linker optimized glutamate-sensitive fluorescent reporters. *Proc. Natl. Acad. Sci. USA* **105**, 4411–4416 (2008).
9. Marvin, J. S. et al. An optimized fluorescent probe for visualizing glutamate neurotransmission. *Nat. Methods* **10**, 162–170 (2013).
10. Borghuis, B. G., Looger, L. L., Tomita, S. & Demb, J. B. Kainate receptors mediate signaling in both transient and sustained OFF bipolar cell pathways in mouse retina. *J. Neurosci.* **34**, 6128–6139 (2014).
11. O’Herron, P. et al. Neural correlates of single-vessel haemodynamic responses in vivo. *Nature* **534**, 378–382 (2016).
12. Brunert, D., Tsuno, Y., Rothermel, M., Shipley, M. T. & Wachowiak, M. Cell-type-specific modulation of sensory responses in olfactory bulb circuits by serotonergic projections from the raphe nuclei. *J. Neurosci.* **36**, 6820–6835 (2016).
13. Helassa, N. et al. Ultrafast glutamate sensors resolve high-frequency release at Schaffer collateral synapses. *Proc. Natl. Acad. Sci. USA* **115**, 5594–5599 (2018).
14. Wu, J. et al. Genetically encoded glutamate indicators with altered color and topology. *ACS Chem. Biol.* **13**, 1832–1837 (2018).
15. Marvin, J. S. et al. Stability, affinity, and chromatic variants of the glutamate sensor iGluSnFR. *Nat. Methods* **15**, 936–939 (2018).
16. Miesenbock, G., De Angelis, D. A. & Rothman, J. E. Visualizing secretion and synaptic transmission with pH-sensitive green fluorescent proteins. *Nature* **394**, 192–195 (1998).
17. Granseth, B., Odermatt, B., Royle, S. J. & Lagnado, L. Clathrin-mediated endocytosis is the dominant mechanism of vesicle retrieval at hippocampal synapses. *Neuron* **51**, 773–786 (2006).
18. Fernández-Alfonso, T., Kwan, R. & Ryan, T. A. Synaptic vesicles interchange their membrane proteins with a large surface reservoir during recycling. *Neuron* **51**, 179–186 (2006).
19. Voglmaier, S. M. et al. Distinct endocytic pathways control the rate and extent of synaptic vesicle protein recycling. *Neuron* **51**, 71–84 (2006).
20. Li, H. Concurrent imaging of synaptic vesicle recycling and calcium dynamics. *Front. Mol. Neurosci.* **4**, 1–10 (2011).
21. Li, Y. & Tsien, R. W. pHTomato, a red, genetically encoded indicator that enables multiplex interrogation of synaptic activity. *Nat. Neurosci.* **15**, 1047–1053 (2012).
22. Rose, T., Schoenenberger, P., Jezek, K. & Oertner, T. G. Developmental refinement of vesicle cycling at Schaffer collateral synapses. *Neuron* **77**, 1109–1121 (2013).
23. Balaji, J. & Ryan, T. A. Single-vesicle imaging reveals that synaptic vesicle exocytosis and endocytosis are coupled by a single stochastic mode. *Proc. Natl. Acad. Sci. USA* **104**, 20576–20581 (2007).
24. Gandhi, S. P. & Stevens, C. F. Three modes of synaptic vesicular recycling revealed by single-vesicle imaging. *Nature* **423**, 607–613 (2003).
25. Zhu, Y., Xu, J. & Heinemann, S. F. Synaptic vesicle exocytosis-endocytosis at central synapses. *Commun. Integr. Biol.* **2**, 418–419 (2009).
26. Maschi, D. & Klyachko, V. A. Spatiotemporal regulation of synaptic vesicle fusion sites in central synapses. *Neuron* **94**, 65–73.e3 (2017).

27. Betz, W. J. & Bewick, G. S. Optical analysis of synaptic vesicle recycling at the frog neuromuscular junction. *Science* **255**, 200–203 (1992).
28. Laviv, T. et al. Simultaneous dual-color fluorescence lifetime imaging with novel red-shifted fluorescent proteins. *Nat. Methods* **13**, 989–992 (2016).
29. Campbell, R. E. et al. A monomeric red fluorescent protein. *Proc Natl. Acad. Sci. USA* **99**, 7877–7882 (2002).
30. Gee, C. E., Ohmert, I., Wiegert, J. S. & Oertner, T. G. Preparation of slice cultures from rodent hippocampus. *Cold Spring Harb. Protoc.* **2017**, 094888 (2017).
31. Pologruto, T. A., Sabatini, B. L. & Svoboda, K. ScanImage: flexible software for operating laser scanning microscopes. *Biomed. Eng. Online* **2**, 13 (2003).
32. Suter, B. A. et al. Ephus: multipurpose data acquisition software for neuroscience experiments. *Front. Neural Circuits* **4**, 1–12 (2010).
33. Negrean, A. & Mansvelder, H. D. Optimal lens design and use in laser-scanning microscopy. *Biomed. Opt. Express* **5**, 1588–1609 (2014).
34. Jensen, T. P., Zheng, K., Tyurikova, O., Reynolds, J. P. & Rusakov, D. A. Monitoring single-synapse glutamate release and presynaptic calcium concentration in organised brain tissue. *Cell Calcium* **64**, 102–108 (2017).
35. Hires, S. A., Zhu, Y. & Tsien, R. Y. Optical measurement of synaptic glutamate spillover and reuptake by linker optimized glutamate-sensitive fluorescent reporters. *Proc. Natl. Acad. Sci. USA* **105**, 4411–4416 (2008).
36. de Lorimier, R. M. et al. Construction of a fluorescent biosensor family. *Protein Sci.* **11**, 2655–2675 (2002).
37. Wiegert, J. S., Gee, C. E. & Oertner, T. G. Single-cell electroporation of neurons. *Cold Spring Harb. Protoc.* **2017**, 135–138 (2017).
38. Luisier, F., Vonesch, C., Blu, T. & Unser, M. Fast interscale wavelet denoising of Poisson-corrupted images. *Signal Process.* **90**, 415–427 (2010).
39. Taschenberger, H., Woehler, A. & Neher, E. Superpriming of synaptic vesicles as a common basis for inter-synapse variability and modulation of synaptic strength. *Proc. Natl. Acad. Sci. USA* **113**, E4548–E4557 (2016).
40. Oertner, T. G., Sabatini, B. L., Nimchinsky, E. A. & Svoboda, K. Facilitation at single synapses probed with optical quantal analysis. *Nat. Neurosci.* **5**, 657–664 (2002).
41. Grabner, C. P. & Moser, T. Individual synaptic vesicles mediate stimulated exocytosis from cochlear inner hair cells. *Proc. Natl. Acad. Sci. USA* **115**, 12811–12816 (2018).
42. Helassa, N., Podor, B., Fine, A. & Török, K. Design and mechanistic insight into ultrafast calcium indicators for monitoring intracellular calcium dynamics. *Sci. Rep.* **6**, 38276 (2016).
43. Zucker, R. S. & Regehr, W. G. Short-term synaptic plasticity. *Annu. Rev. Physiol.* **64**, 355–405 (2002).

Acknowledgements

We thank I. Ohmert and S. Graf for the preparation of organotypic cultures and excellent technical assistance. This study was supported by the German Research Foundation through Research Unit FOR 2419 P4 (T.G.O.) and P7 (J.S.W.), Priority Programs SPP 1665 (T.G.O.) and SPP 1926 (J.S.W.), Collaborative Research Center grant SFB 936 B7 (T.G.O.), and BBSRC grants BB/M02556X/1 (K.T.) and BB/S003894 (K.T.). We thank R. Y. Tsien (University of California, San Diego) for providing pCI syn tdimer2.

Author contributions

C.D.D., J.S.W., K.T., and T.G.O. designed the experiments and prepared the manuscript. C.D.D. performed synaptic imaging experiments. N.H., S.K., C.C., and M.G. created and characterized novel iGluSnFR variants, C.S. wrote software to acquire and analyze GEG data.

Competing interests

The authors declare no competing interests.

Additional information

Supplementary information is available for this paper at <https://doi.org/10.1038/s41596-019-0143-9>.

Reprints and permissions information is available at www.nature.com/reprints.

Correspondence and requests for materials should be addressed to T.G.O.

Journal peer review information: *Nature Protocols* thanks Edwin R. Chapman, Yulong Li, Jason Vevea and other anonymous reviewer(s) for their contribution to the peer review of this work.

Publisher's note: Springer Nature remains neutral with regard to jurisdictional claims in published maps and institutional affiliations.

Received: 8 October 2018; Accepted: 22 January 2019;

Published online: 15 April 2019

Related links

Key reference using this protocol

Helassa, N. et al. *Proc. Natl. Acad. Sci. USA* **115**, 5594–5599 (2018): <https://www.pnas.org/content/115/21/5594>